

Review

Dissecting the Inorganic Nanoparticle-Driven Interferences on Adhesome Dynamics

Vladimir Mulens-Arias

Integrative Biomedical Materials and Nanomedicine Lab, Department of Experimental and Health Sciences (DCEXS), Pompeu Fabra University, PRBB, Carrer Doctor Aiguader 88, 08003 Barcelona, Spain; vladimir.mulens@upf.edu; Tel.: +34-933-160-917

Abstract: Inorganic nanoparticles have emerged as an attractive theranostic tool applied to different pathologies such as cancer. However, the increment in inorganic nanoparticle application in biomedicine has prompted the scientific community to assess their potential toxicities, often preventing them from entering clinical settings. Cytoskeleton network and the related adhesomes nest are present in most cellular processes such as proliferation, migration, and cell death. The nanoparticle treatment can interfere with the cytoskeleton and adhesome dynamics, thus inflicting cellular damage. Therefore, it is crucial dissecting the molecular mechanisms involved in nanoparticle cytotoxicity. This review will briefly address the main characteristics of different adhesion structures and focus on the most relevant effects of inorganic nanoparticles with biomedical potential on cellular adhesome dynamics. Besides, the review put into perspective the use of inorganic nanoparticles for cytoskeleton targeting or study as a versatile tool. The dissection of the molecular mechanisms involved in the nanoparticle-driven interference of adhesome dynamics will facilitate the future development of nanotheranostics targeting cytoskeleton and adhesomes to tackle several diseases, such as cancer.

Keywords: adhesome; cytoskeleton; inorganic nanoparticle; migration; invasion



Citation: Mulens-Arias, V. Dissecting the Inorganic Nanoparticle-Driven Interferences on Adhesome Dynamics. *J. Nanotheranostics* **2021**, *2*, 174–195. <https://doi.org/10.3390/jnt2030011>

Academic Editor: Moein Moghimi

Received: 22 July 2021

Accepted: 13 August 2021

Published: 2 September 2021

Publisher's Note: MDPI stays neutral with regard to jurisdictional claims in published maps and institutional affiliations.



Copyright: © 2021 by the author. Licensee MDPI, Basel, Switzerland. This article is an open access article distributed under the terms and conditions of the Creative Commons Attribution (CC BY) license (<https://creativecommons.org/licenses/by/4.0/>).

1. Introduction

The nanomedicine field has grown in the last decades, supported by the development of highly innovative and easy-to-scale nanomaterials to treat diverse pathologies, e.g., cancer [1–4], autoimmune [5,6], and neurodegenerative disorders [7,8]. The therapeutic success of nanomaterials, in particular nanoparticles, relies on the relatively low toxicity and the chemical and physical versatility that facilitate their functionalization. Researchers have modified nanoparticle surfaces with a variety of moieties such as targeting moieties [9], drugs [10], the on-surface-built stimuli-responsive molecular domains, e.g., pH- [11,12], and reactive oxygen species (ROS)-sensitive bonds [13,14]. Combining the above surface domains with the intrinsic physical properties associated with nanoparticle core, such as magnetism [15] and plasmon coupling [16], provides promising tools for therapy and diagnosis. Nonetheless, nanotoxicological concerns remain the bottleneck hurdle for nanotheranostics to reach clinical stages [15–17]. For the wide range of potentially toxic biological outcomes that cells can undergo upon nanoparticle-cell interaction, the cytoskeleton-associated disarrangements play a key role in mediating these processes. Biological processes such as cell migration [18], invasion [19], immune response [20,21], proliferation [22], and cell death [23], depend partly or entirely on the dynamics of cytoskeleton-stemmed structures. However, only recently has some research addressed the complexity of cytoskeleton–nanoparticle interactions, becoming an active and vital field for nanotheranostic development. We will discuss and put into perspective the recent advancements in this matter. At first glance, we will highlight the adhesive structures' main structural and functional features focusing on similarities and disparities. We then revise and discuss the effect of different inorganic nanoparticles on adhesive structures

and consider the importance of elucidating nanoparticle interference with cytoskeleton dynamics.

2. Adhesome Structure, Function, and Dynamics

The term adhesome collectively refers to a complex structural domain that links the intracellular cytoskeleton network to the adhesion complexes and the protein network interactions comprising such domains [24,25]. These proteins act as a scaffold for the formation of adhesions and integrate the extracellular signals into a rapid functional response regulated by kinases, GTPases, and proteolytic enzymes. Adhesome definition was first coined by Singer II, et al. referring to granules containing extracellular matrix (ECM)-specific receptors in leukocytes and monocytes [26]. However, the term expanded to include the entire protein network comprising or regulating all the cell-ECM interactions and the cell-cell and the cell-matrix adhesion receptors [27]. The structures that mediate the cell-ECM adhesions include filopodia [28], lamellipodia [29], focal adhesions [30], podosomes [31], and invadopodia [32], all differing in protein composition, dynamic, and functional activity, often associated with a specific cell type and microenvironmental context [31]. Significant structural and functional differences between these structures highlight the high complexity of the cell-ECM interaction (Table 1). We briefly pinpoint the principal structural components and the functions of these actin-rich microdomains.

Filopodia and lamellipodia are related structures. Filopodia arise from lamellipodia upon actin rearrangement into parallel filaments bundled by actin-bundling proteins, i.e., fascin, villin, and α -actinin (Figure 1). Numerous actin-capping proteins such as formin [33,34], small GTPases belonging to Rho families such as Rac1 and Cdc42 [35,36], kinases [37], and actin regulators such as Ena/Vasp [38,39], facilitate the actin linear polymerization. Filopodia are sensitive to mechanical forces that ultimately regulate their dynamics and seemingly depend on formin and myosin IIA interplay at the filopodium base [40]. Noteworthy, actin-bundling proteins tightly pack actin filament in a unidirectional manner, allowing the motor machinery to transport receptors and vesicles toward the tip of the filopodium. Filopodia are mediators of cell probing of the surrounding microenvironment in various physiological processes such as immune response [41] and embryonic development [42] due to their structural organization and the unidirectional transport of receptors. Since filopodia act as transport tunnels for receptors, e.g., integrins, they drive the formation of adhesions at diverse locations within the structure. Those at the base of the tip are more similar to the focal adhesions formed at the lamellipodia.

Nonetheless, those assembled at the filopodia shaft and the end are less characterized. They likely play an essential role in stabilizing the filopodium and probing or reinforcing the cell-cell junctions and cell-ECM anchorage, limiting the filopodium growth [43] and the sensing of the ECM rigidity [44]. What is certain is that the cyclic lamellipodium advancement and retraction promote the formation of these adhesions at the filopodium shaft. Some reports, however, indicate that the adhesions formed at the shaft and the tip of the filopodium can evolve toward a mature focal adhesion, suggesting that the former are more like nascent focal adhesions [44].

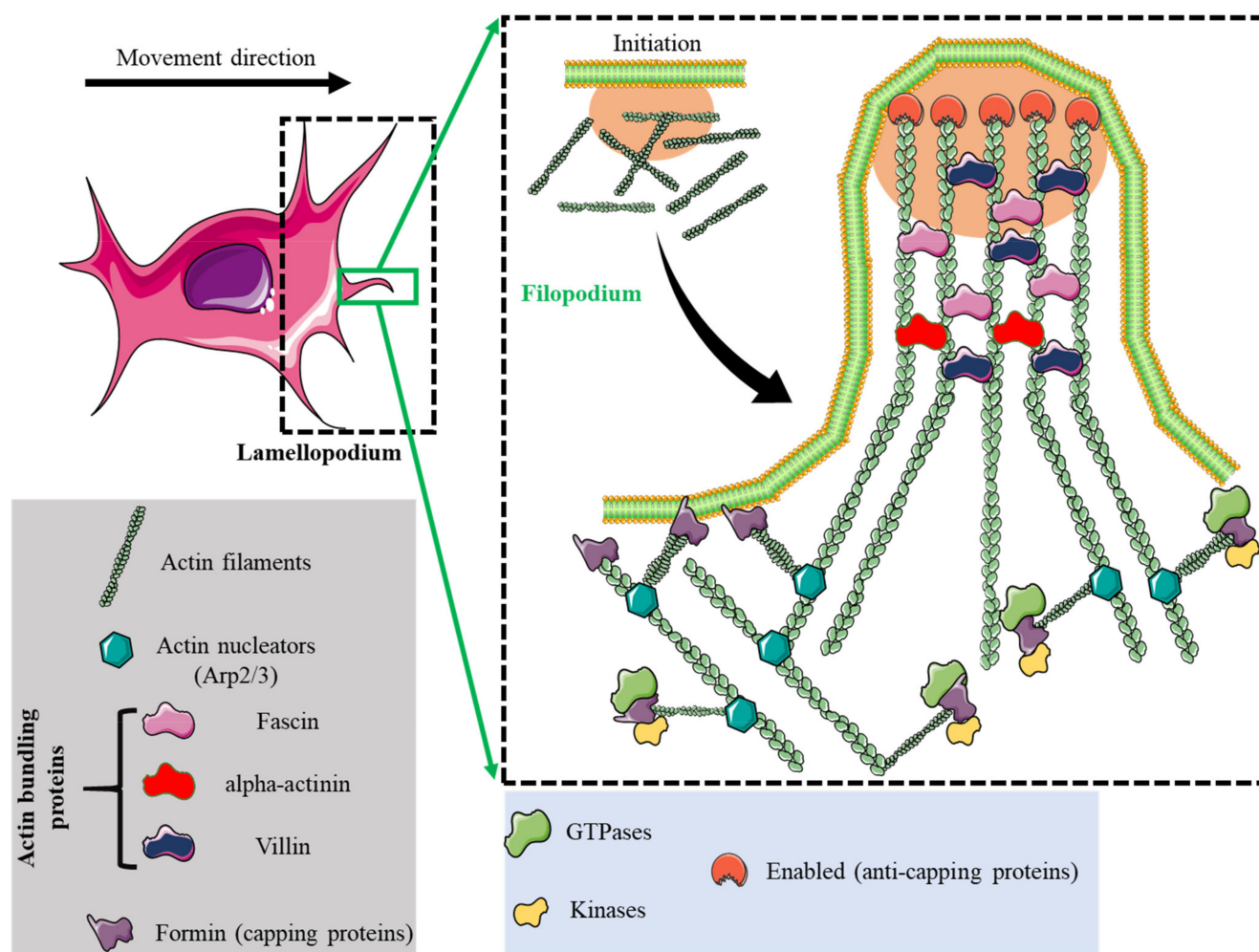


Figure 1. Actin rearrangement in lamellipodia and filopodia. Filopodia emerge from lamellipodium at the leading edge in a cell in movement. Then, actin starts nucleating, helped by specialized proteins such as Arp2/3, GTPases, kinases, and regulators of the actin polymerization such as capping (formin) and anti-capping (Enabled) proteins, these last allowing filament growth, protruding into filopodial extensions. Concomitantly, actin-bundling proteins such as fascin, villin, and α -actinin, bundle actin filaments.

Table 1. Adhesive structures, connecting cytoskeleton with ECM, structural and functional differences.

	Lamellipodia	Filopodia	Focal Adhesions	Podosomes	Invadopodia
Structure	Sheet-like protrusions that attach to ECM driven by branched actin arrangements	Often originating at lamellipodium as finger-like extensions driven by linear actin polymerization	Clusters of transmembrane receptors, integrins, and cytosolic proteins driven by parallel actin filaments branched at the end	A discrete actin-rich core surrounded by a ring of actin-associated and signaling proteins, driven by branched and unbranched actin filaments	A discrete actin-rich core is surrounded by a ring of actin-associated and signaling proteins. Often linked to tumor cells driven by parallel actin filaments within the tip and branched at the base
Cellular location	Leading-edge	Embedded within lamellipodia	Leading-edge of the cell	Ventral cell surface, often clustered behind the leading edge of the cell	Ventral cell surface, often situated under the nucleus

Table 1. Cont.

	Lamellipodia	Filopodia	Focal Adhesions	Podosomes	Invadopodia
Dimesions	Width: 0.1–0.2 μm	Width: 0.1–0.3 μm ; length: 3–10 μm	Width: 2–6 μm	Width: 0.5–2 μm ; length: 0.5–1 μm [45]	Width: 0.5–2 μm ; length: >2 μm
Pericellular proteolysis	Minimal	No	Minimal [46]	Yes, through MT1MMP and UPAR	Yes, through MMP2, MMP9, MT1MMP, seprase, UPAR, ADAM12, ADAM15, and ADAM19
Duration of structure	Minutes	Minutes	Hours, it depends on the rate of cell migration	Minutes [47]	Hours [48]
Soluble stimuli	HGF [49,50], TNF α and TNF β [51], endothelin-3 [52], CLCF-1 [53]	VEGF-A [54], GDF-5 [55], EGF [56], HGF [57], TNF α [58] and TNF β [51], leptin [59]	Estrogen [60], TGF β 1 [61], endothelin-3 [52]	IL-5 [62], VEGF-A [63], pro-NGF [64], thymosin α 1 [65], hepatoma-derived growth factor (HDGF) [66], TGF β 1 [67], NaF [68], KGF [69], SDF-1 α [70], exosomes [71], osteopontin [72]	EGF [73], PDGF [74], TGF β [75], VEGF [76], HGF [77,78], SDF-1 [79]
ECM stimuli	Fibronectin [80], fibrinogen [81]	Fibronectin [80], fibrinogen [81]	Fibronectin [82,83],	Collagen I [84], fibronectin [85,86], fibrinogen [85],	Fibrinogen [87], Collagen I [88,89], hyaluronan [90]

Focal adhesions (FAs) are membrane microdomains that cluster transmembrane receptors, i.e., integrins and a plaid of cytosolic proteins involved in scaffolding, actin arrangement, and regulatory activities [91] (Figure 2). FAs are actin-rich structures specialized in transducing mechanical cues into biochemical signals where focal adhesion kinase (FAK) plays a central role acting as a signaling hub between transmembrane receptors and downstream proteins [92,93]. The translocation of FAK to FAs requires the autophosphorylation of FAK (Tyr397), which opens an Src homology 2 (SH2) binding site for the kinase Src to associate, and, in turn, phosphorylate other residues at the kinase domain activation loop of FAK (Tyr576/577). Afterward, the formation of the Src-FAK complex renders the maximal activation status of FAK, facilitating the phosphorylation of other sites at the FAT domain and recruiting several downstream proteins targeted to the FA [94]. The physical interaction between integrins and ECM elements allows the sensing of mechanical forces at the cell-ECM interface, triggering a series of biochemical reactions that modulate the intracellular cytoskeleton [95].

Although it is well known that FAs mediate outside-in (ECM-stemmed) signaling, FAs can also mediate inside-out signaling (cytoskeleton-stemmed). Indeed, the intracellular traction forces driven by actomyosin are transferred to the ECM through FAs [96]. FAK and paxillin [97], and other proteins, are part of the signaling module of the FA adhesome. The structural module comprises proteins involved in FA stabilization and maturation and includes three major components: vinculin, talin, and tensin [98]. It is noteworthy that the structural proteins' turnover exhibit a more prominent dependence on ECM stiffness than signaling proteins [99], emphasizing their role as mechanosensing mediators. The interplay between ECM and intracellular traction forces is mediated by several mechanosensitive proteins that respond to tension-triggered conformational changes. Their targeting, residence time, and turnover at the FA appear to depend on the magnitude of ECM stiffness. Of all, vinculin and paxillin constitute fundamental partners in bridging mechanobiological transduction at FAs [100]. However, vinculin also promotes FA maturation, which correlates with the sensing of external stiffness [101]. Vinculin cooperates with another

essential actin-binding protein, talin, to provide FA stabilization and, therefore, FA maturation [102,103]. Accordingly, the FERM domain-containing talin head interacts with the short intracellular tail of the β -integrin subunit, thus releasing the α -integrin subunit from its inhibitory effects and inducing conformational changes in the extracellular domains that increase integrin affinity for their ligands [104].

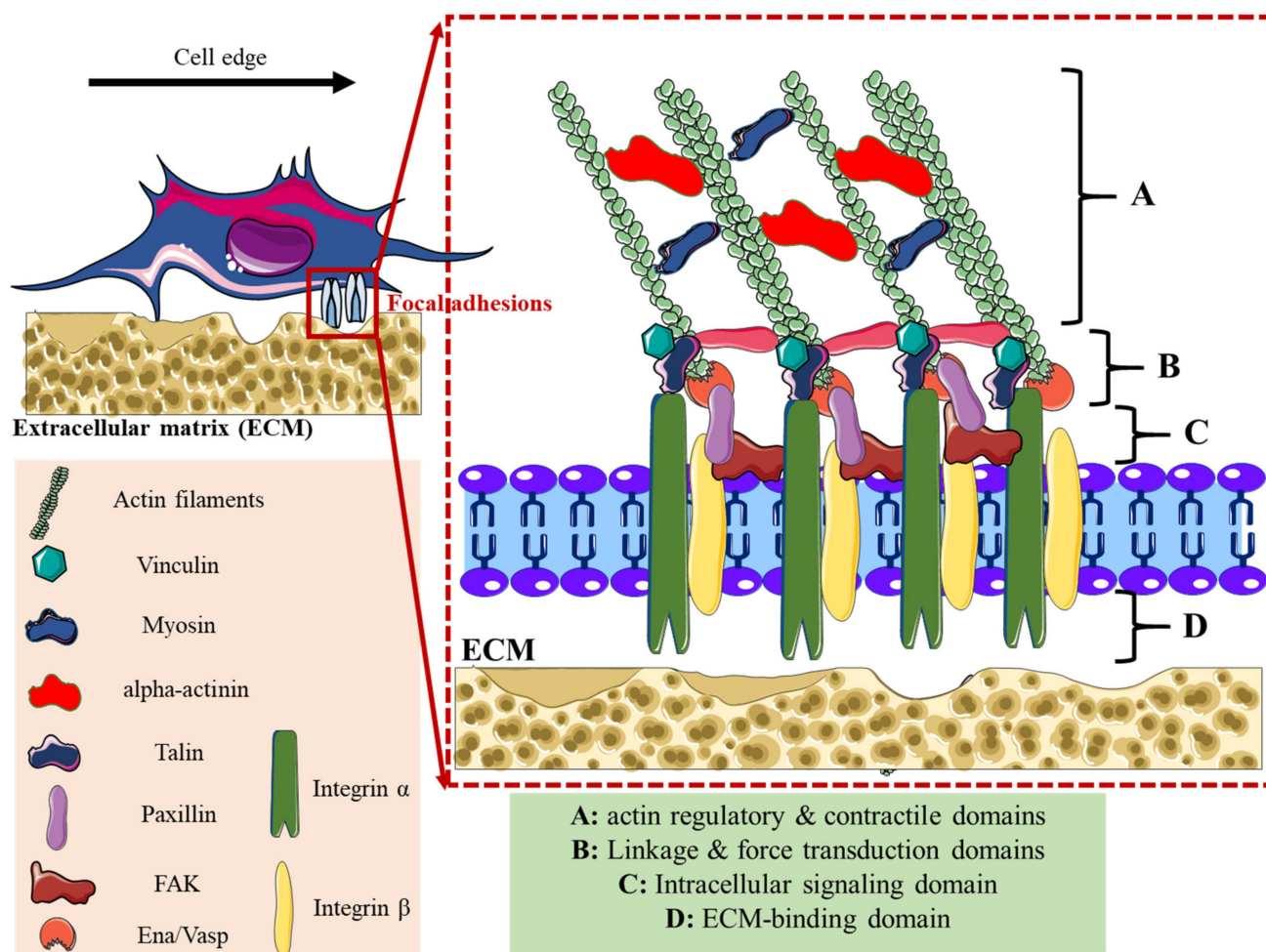


Figure 2. Schematic representation of focal adhesion structure and the different molecular domains. FA mediates the ECM-cell contact through integrin receptors (domain D). The integrin–integrin receptor engagement triggers the recruitment of critical kinases, such as FAK (domain C), to transduce the signal into structural changes in actin-linking proteins (domain B). As a result, the extracellular signal promotes actin filament mechanical force (domain A). The schematic simplifies the complex FA machinery to include those proteins that are most likely to be involved in the formation and structural integrity of FAs.

The invadosome family comprises two multi-molecular complexes at the cytoplasmic membrane: podosomes, found in a physiological context such as immune response, and invadopodia, described in pathological scenarios as cancer. While FAs anchor cells to ECM, invadosomes degrade ECM to facilitate cell migration through tissue and basement membrane. Podosomes, like FAs, contain integrins that help cells probe ECM stiffness in an outside-in signaling process. In contrast to FAs, podosomes provide cells with ECM degradation ability through the focalized secretion of metalloproteases and other proteases (Figure 3). A microtubule/motor-mediated vesicular transport at the site of podosome core often confines proteases such as the membrane-bound MT1-MMP [47,105,106], maintaining an on-demand proteolytic reservoir (Table 1 and [107]). Podosomes are dot-like actin-rich structures often found as individual dots, clusters, belt-arranged formations

in steady cells. External cues such as ECM stiffness or cytokine/growth factors induce podosomes to re-arrange into ring-like sealing areas called rosettes [31]. Noteworthy, the coalescence of individual podosomes and the fission of larger rosettes drive the de novo formation of podosome superstructures, most likely through the polarization of myosin II-mediated contractility [108]. From a structural point of view, podosomes can be described as a modular architecture, consisting of two different parts: (1) an actin-rich protrusive core driven by the Arp2/3-mediated actin polymerization, and (2) an integrin-based discontinuous cluster-like ring that surrounds the core [109]. Curiously, the distribution appears to follow an isotype-specific localization within the podosome structure with $\beta 1$ associated with the core, whereas both $\beta 2$ and $\beta 3$ localize in the ring preferably [45,110,111]. The ability of podosome to re-arrange into a more complex superstructure relies on a set of two unbranched actin filaments, i.e., the ventral lateral filaments that likely connect integrin and another adhesive receptors-based ring with the branched actin-rich core [47], and the dorsal filaments most likely involved in linking individual podosomes to form clusters, belt, or rosettes [112,113]. Nonetheless, a newly discovered set of filaments in dendritic cells can be involved in the podosome arrangement into superstructures, i.e., interpodosomal zyxin-positive filaments that appear to bring podosomes close and do not depend on actin polymerization [114]. Podosome cap is another structural module that hubs actin- and myosin-interacting protein, regulates its activity, and is linked to contractility forces. Besides, podosome caps are the primary source of podosome variability even within a single cell. In macrophages, a larger podosome population at the leading edge coexists with other smaller podosome subpopulations of a longer life in the ventral zone of the cells [115]. Similar to FAs, actin-linkers proteins are also found within podosomes, including paxillin [116], vinculin [117], and talin [118]. Noteworthy, ECM can drive podosome formation and dictate which integrin responds on a cell-type bias (e.g., $\beta 1$ binds collagen I in megakaryocytes [85], $\beta 2$ binds fibrinogen in macrophages [119], and $\beta 3$ binds osteopontin in osteoclasts [120]) and also the ECM fiber geometry can influence podosome subcellular localization, morphology, rearrangement, and lifetime [85,109,121]. That is the case for dendritic cells where interpodosomal filaments-driven arrangement into highly packed clusters is dictated by substrate topology [114]. Therefore, podosomes are highly dynamic actin-rich structures whose architecture, morphology, configuration, localization, and proteolytic activity are dictated by both intracellular dynamical cytoskeleton-stemmed forces and the composition and organization of the ECM.

As mentioned before, invadopodia associate with diverse pathological conditions such as cancer. They are the main ECM-degrading structures that mediate tumor cell invasion and metastasis [122–124] and, therefore, are one of the potential targets for cancer treatment [125]. Although invadopodia share structural similarities and components with podosomes, they exhibit a more extended life even for hours [50] than their counterparts, which usually last less than 10 min [47,126,127]. Like podosomes, invadopodia are also protrusive structures that elongate deeper in the ECM. In terms of protein composition, invadopodia and podosomes show proven differences. For instance, the regulatory proteins WASP and Grb2 locate at podosomes but not at invadopodia [128,129], while Nck1 and the ENA/Vasp family member Mena (mammalian-ENA) protein form part of invadopodia but not podosomes [130–132]. The currently accepted model for invadopodium formation distinguishes three discrete temporal stages, i.e., (I) invadopodium core precursor initiation triggered by ECM or growth factors, (II) invadopodium core precursor stabilization, and (III) invadopodium maturation. For invadopodium to start forming, actin-nucleation proteins, such as Arp2/3, cofilin, and regulatory protein N-WASP, must translocate to and associate with the nascent cortactin-actin complexes close to the plasma membrane. Following phosphorylation of cortactin, the complex Nck1-N-WASP supports the limited Arp2/3-dependent actin polymerization. The nascent invadopodium core precursor stabilization is then driven by the Src kinase substrate, Tks5, which anchors the core to the plasma membrane through PI(3,4)P2 [48]. The recruitment of PI(3,4)P2-producing phosphatase SHIP2 by lamellipodin-Mena complex [133,134] further strengthens the Tks5-

dependent invadopodium core [118]. Such recruitment is facilitated by a PH domain within lamellipodin, driving its anchoring to the plasma membrane [135]. The actin polymerization initiation attracts the myosin II- Na^+/H^+ exchanger-1 (NHE1) complex, lowering local pH and activating cofilin-dependent actin polymerization [136]. Both actin-polymerization mechanisms then synergize in growing the membrane protrusion. Cofilin drives the formation of daughter actin filaments that in turn activate new N-WASP-Arp2/3-mediated actin nucleation [136]. Invadopodium maturation is finally forced by the Small GTPase Cdc42 that keeps Arp2/3 complex activated, and thereby the elongation of the filaments and the protrusion growth [137,138]. An active vesicular transport toward protrusions occurs, mediating the secretion of proteolytic enzymes that degrade the basement membrane and ECM [139]. In this regard, Tks5 also plays a key role by tethering the Rab GTPase Rab40b-positive MMP2- and MMP9-containing vesicles through its PX domain. Consequently, vesicles are targeted to invadopodia, and the proteolytic content is released into the extracellular microenvironment [140]. The metalloproteinase MT1-MMP trafficking toward invadopodia seems to be mediated by other vesicular trafficking molecules such as syntaxin 4 and the vesicle-associated membrane protein 7 (VAMP7) [141,142]. Although the initiation of invadopodia can occur in seconds to minutes, their maturation and stabilization can last for hours allowing tumor cells to degrade ECM and invade surrounding tissues.

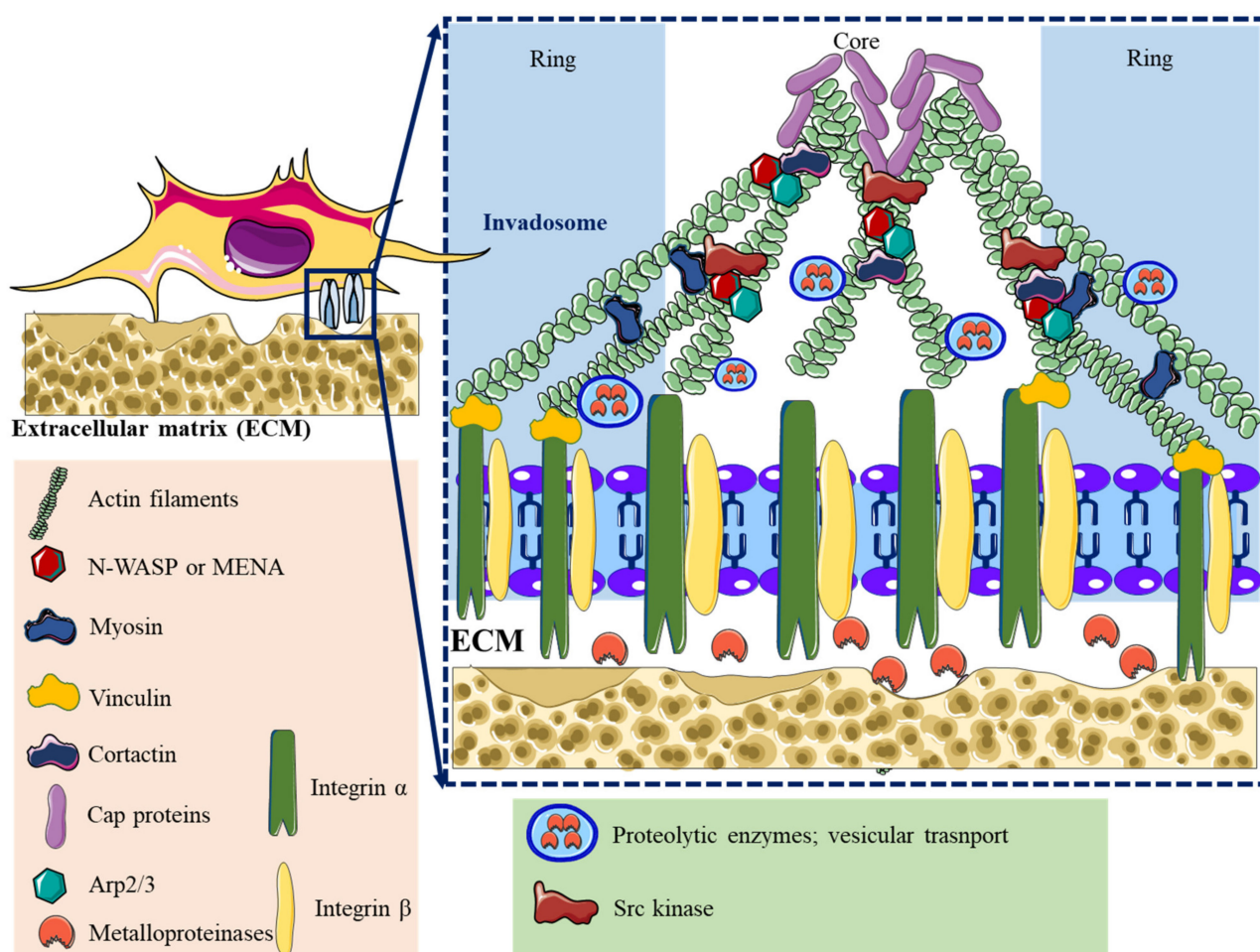


Figure 3. Schematic representation of invadosome (podosomes and invadopodia). Invadosomes mediate the ECM degradation through the secretion of several metalloproteinases and other proteases. The schematic simplifies the complex invadosome machinery to include those proteins that are most likely to be involved in its formation and structural integrity.

3. Impact of Inorganic Nanoparticles on Adhesome Dynamics

The extended biomedical application of metallic nanoparticles and the underlying concern on their effects on living systems from the cell to the organism level have raised the need to better understand the complex interaction with cell processes. The nanoparticle internalization requires the mobilization of the endocytosis machinery, which in turn triggers cytoskeleton arrangements. Therefore, the endocytosis of nanoparticles per se affects the cytoskeleton dynamics and all the associated cellular structures indirectly. Once inside the cells, the nanoparticles can trigger a broad spectrum of cellular signaling pathways depending on their chemical nature, including those affecting the cytoskeleton dynamics. To better guide the readers, the effect of nanoparticles on adhesomes will be classified according to the signaling input: (1) as outside-in when the interaction of nanoparticles with the cell membrane induces profound changes in adhesome dynamics, thus being a ECM-stemmed signal; and (2) inside-out, when internalized, the nanoparticles activate diverse signaling pathways leading to a profound change in adhesome dynamics, thus being a cytoskeleton-stemmed signal (Table 2). This classification will allow us to dissect whether the interaction of the nanoparticles with cell membrane microdomains is sufficient for disturbing adhesomes or whether intracellular trafficking and biodegradation of nanoparticles are needed to promote such changes.

3.1. Inorganic Nanoparticles and Focal Adhesions Dynamic

Nanoparticle-induced disturbance of cytoskeleton arrangement would potentially affect cytoskeleton-based cellular processes such as migration and invasion. Indeed, Vieira et al. observed that human fibroblasts subjected to AuNP or AgNP exhibited increased intracellular actin fibers correlating with a significant migration impairment [143]. Although no further elucidation of the molecular machinery behind such effect was performed, it was clear that inorganic nanoparticles impacted cytoskeleton dynamics. Soon after, Lo HM et al. demonstrated that similar AuNP could disrupt platelet-derived growth factor (PDGF)-induced FAK phosphorylation, decreasing the vascular smooth muscle cell adhesion to a collagen I-rich ECM and inhibiting cell migration [144]. Recently, Kráľovec K., et al. observed that a novel type of complex nanoparticles, SiO₂@Ga-substituted ε-Fe₂O₃, also induced FA shortening and a loss of stress fibers in human lung adenocarcinoma A549 [145]. Therefore, inorganic nanoparticles disturb fiber formation and stability at first glance, leading to an impaired cell migration. Table 2 summarizes the more recent reports on inorganic nanoparticle effects on FA dynamics.

An important aspect when studying the effect of nanoparticles on cell migration is the experimental system adopted. The latter should resemble as far as possible the biological microenvironment where the cells in question nest. In this regard, glioblastoma cells U87 migration appeared unaffected when treated with transferrin-coated porous silica nanoparticles (Tf@SiNP) in the classical 2D wound scratch experimental setup. Nonetheless, Tf@SiNP did inhibit U87 migration within a microfluidic chamber that mimics the tight ECM tract found in tumor masses [146]. Noticeably, migrating cells exhibited a shortened FA dynamics at the leading edge where FAs disassembled after 20 min compared to the 50 min of persistent FA formation in untreated cells [146]. Cells also lost plasticity, as suggested by the loss of cell volume, which precludes them from properly shrink from entering microfluidic chambers.

Cell adhesive capacity, often detrimental to cell migration, might be beneficial in certain physiological and pathological conditions. That is the case for human mesenchymal stem cell (hMSC)-based therapy for heart infarction. For hMSCs to properly adhere to ventricles walls, FAs must exhibit a highly stabilized structure that lasts enough for cells to reach the infarcted tissue. In this sense, Popara, et al. found that hMSCs treated with SiO₂ NP display more elongated and more oversized FAs that consistently favored hMSCs stronger adhesion to fibronectin-based ECM in vitro. More importantly, when injected in heart infarcted rats, SiO₂ NP-treated hMSCs grafted more in both ventricles walls than untreated counterparts [147]. Although the authors did not elucidate precisely which

molecular pathways might underly the SiO₂ NP effect on FAs, the fact that SiO₂ NP-treated hMSCs showed transiently impaired autophagy might as well explain the slow FA turnover. Autophagy is integral to the degradation of several components of FA structure and integrin trafficking system mediated by the autophagy cargo receptor NBR1 [148–150]. Consequently, cells where autophagy is impaired display an enlarged leading edge-stemmed FAs due to the slow assembly-disassembly rate [150,151]. Therefore, the nanoparticle can disturb proper FA dynamics indirectly by damaging autophagy-dependent FA turnover. Indeed, many inorganic nanoparticles can interfere with autophagy processes by fostering or inhibiting them. However, most of these studies do not address whether cell adhesions are affected. The direct involvement of autophagy in FA turnover has become a potential target for metastasis, as demonstrated by Wang, Y. et al., who designed a tumor-activable nanoparticle carrying the autophagy inhibitor chloroquine. Nanoparticle-treated 4T1 tumor cells exhibited a >2 fold decrease in paxillin degradation in vitro and in vivo and consequently displayed a reduced migration and metastatic potential [152].

Nonetheless, Shin, T.H. et al. were able to elucidate the molecular signaling engaged upon silica-coated magnetic nanoparticle internalization in human bone marrow-derived mesenchymal stem cells (hBM-MSCs). That is: SiO₂@MNP induced a significant cell shrinkage along with a consistent loss of FAs and reduced traction forces [153]. The diminished phosphorylation of FA-associated kinases such as FAK and Src reflected an intrinsic inability to form FA properly. Interestingly, Shin, T.H. et al. observed that SiO₂@MNP treatment hamper cell membrane fluidity mediated by increased lipid oxidation. Therefore, reactive oxygen species (ROS)-mediated mechanisms can partially contribute to the global effect of nanoparticles on cytoskeleton dynamics. Indeed, Mulens-Arias, V. et al. also found ROS can mediate nanoparticle-induced FA disturbance. Polyethyleimine@IONP-treated human umbilical vein endothelial cells (HUVECs) showed a reduced FA number concomitant with a decrease in phosphorylated Src and phosphorylated cortactin. However, when cells were pre-treated with the ROS-scavenger BHA, phosphorylated Src and cortactin levels were recovered [154]. This change in cytoskeleton morphology has also been observed with gold nanoparticles when internalized by HUVECs. More in detail, Ma, X. et al. detected a shortening of actin and tubulin fibers leading to reduced filipodia and FA area [155]. More important, using biochemical cell-free actin and tubulin polymerization assay, AuNP impaired polymerization reactions and the elongation of actin and tubulin fibers in vitro, likely indicating a direct and physical interference with fiber dynamics in cellulo.

Nanoparticle effects on cytoskeleton dynamics often emerge without detectable cell death, at least in a short time, emphasizing the need for in-depth analysis of nanoparticle–cell interaction. Kráľovec, K. et al. found that even when cell death was not detected, yet thiol-functionalized silica-coated IONPs induced a profound disruption of the microtubule network (β -tubulin⁺) and a shortening of the FAs (paxillin⁺) in A549 cells accompanied by the impairment of the spatial organization of the cytoskeletal network and FA-associated proteins [156]. In contrast with the work in hBM-MSCs by Shin, T.H. et al. [153], the thiol-functionalized silica-coated IONPs augmented FAK phosphorylation, suggesting a distinct molecular mechanism for FA disruption.

The dysregulation of filopodia and FA dynamics induced by nanoparticle treatment can lead to a loss in rigidity sensing of the cell. In this regard, Ketebo, A.A. et al. found that SiO₂@MNP reduced the formation of filopodia and FAs in HEK293 cells when seeded onto a rigid surface (2 MPa) but inflicted negligible effect on cells seeded on a soft surface (5 kPa). In addition, it appeared that reduced phosphorylation of paxillin accounts for the impairment of FA formation, leading to a change in the spatial force distribution and directionality at the leading edge of HEK293 cells [157].

There is evidence that, even when focal adhesions do not exhibit a proteolytic activity as high as that of invadosomes (podosomes and invadopodia), FAs can degrade ECM to some extent [46,158]. Therefore, according to the described effects of inorganic nanoparticles on the FA dynamic, it is logical to believe that they can indirectly affect FA-dependent ECM degradation. Indeed, Mulens-Arias, V. et al. found that AuNP of 16, 30, and 40 nm

of diameter induced an increase in FA size in mouse endothelial cells, SVEC4-10, in the first 30 min of incubation followed by a significant reduction after 1 h [159]. As a result, murine endothelial cells degraded less the ECM, most likely due to an impairment of MT-MMP recruitment to FAs, the decrease in MMP2, and the increase of metalloproteinase inhibitors TIMP1 and Serpine1. However, the same AuNPs had the opposite effect on mouse mesenchymal stem cells (mMSCs) as both the total (Vinculin⁺/F-Actin⁺) and the mature (Zyxin⁺/F-Actin⁺) FA number and size increased as early as 1 h after AuNP treatment. Consequently, AuNP-treated mMSCs exhibited an exacerbated ECM degradation rate [159]. These effects were observed at early incubation times (<1 h), suggesting that the mere AuNP interaction with cells effectively affects FA dynamics, thus supporting the outside-in signaling mechanism.

Soenen, S.J.H. et al. found evidence on the physical hindering of intracellular cytoskeleton network analyzing clinical relevant iron oxide nanoparticles (IONPs) such as Resovist and Endorem, and other experimental very small IONPs and magnetoliposomes [160]. When treated with any of these IONPs, the primary human blood outgrowth endothelial cells (hBOECs) exhibit a disrupted cytoskeleton and microtubule architecture accompanied by a reduction in the level of phosphoY358-FAK, thereby impairing FA formation and maturation. Nonetheless, metallic nanoparticles appear to strengthen the actin filament tension by disrupting the tubulin network in some cases. Tay, C.Y. et al. demonstrated that when oral mucosa cells TR146 are treated with TiO₂, SiO₂, and hydroxyapatite nanoparticles, the acetylated α -tubulin, which is responsible for the tubulin network stabilization, decreased, thus exacerbating the intracellular F-actin filament traction forces [161]. Actomyosin and microtubules are antagonistic force-generators that keep the intracellular tensile homeostasis. While the slide of the actomyosin motor along the actin filaments generates contractility, the microtubules counteract this force by generating compressional forces and prevent the cell from collapsing [162–164]. Therefore, if nanoparticles perturb microtubule stability, the contractility will increase accordingly. It is documented that FAs grow and mature partly by the generated intracellular tension when mediating mechanical transmission in an inside-out manner [165,166]. In line with this, Tay, C.Y. et al. found that nanoparticle-treated TR146 cells showed an increase in the formation and maturation of FA, most likely due to the exacerbated tension in filamentous actin filaments and, as a result, cell migration is retarded [161].

Similar sensitivity of microtubule network to metallic nanoparticles was observed by Ibrahim, M. et al. when treated human osteoblast-like cells SaOS-2 with TiO₂ nanoparticles [167]. Despite the global increase in phosphorylated FAK (Tyr397), TiO₂-treated SaOS-2 cells failed to recruit phospho-FAK to FA, reducing their size. Moreover, TiO₂ nanoparticles also downmodulated the level of vinculin, a structural protein tightly linked to FA, partly explaining the reduced FA area. One excellent example of how signaling direction can differentially affect FA dynamic is TiO₂. Contrarily to the TiO₂ nanoparticle internalization effect on FA in osteoblast, osteoblasts cultured on nano-thin TiO₂ surface display an increase in FA size, which exacerbated cell adhesion to the surface [168].

Table 2. List of inorganic nanoparticles and their effect on focal adhesion dynamic.

Nanoparticle	Cell	FA Markers	Probable Signaling Direction	Time (h)	Effect
SiO ₂	Human mesenchymal stem cells	Vinculin	Inside–out	16	Increased FA size and maturation [147]
SiO ₂ (50, 100, 300 nm)	Bovine aortic endothelial cells (BAEC)	F-actin/vinculin	Outside–in	24	Decreased FA size [169]
SiO ₂ (50, 100, 300 nm)	Mouse calvarial preosteoblasts (MC3T3-E1)	F-actin/vinculin	Outside–in	24	Increased FA size [169]
SiO ₂ @IONP	Human bone marrow-derived mesenchymal stem cells (hBM-MSCs)	F-actin/vinculin	Inside–out	12	Decreased FA size, decreased phospho-Src, reduced phospho-FAK, reduced traction forces and cell migration [153]
Ga-substituted ϵ -Fe ₂ O ₃	A549	F-actin/vinculin	Inside–out	24	Decreased FA area and reduced cell adhesion [145]
Resovist, Endorem, and magnetoliposomes	Primary human blood outgrowth endothelial cells (hBOECs)	F-actin/vinculin	Inside–out	24	Decreased FA formation and maturation Reduced phospho-FAK Reduced cell migration [160]
AuNP (16, 30, 40 nm)	Mouse endothelial cell (SVEC4-10)	F-actin/vinculin and F-actin/zyxin	Outside–in	2 and 24	Decreased total FA size, reduced MT1-MMP recruitment Reduced MMP2 and ECM degradation [159]
AuNP (16, 30, 40 nm)	Mouse mesenchymal stem cells	F-actin/vinculin and F-actin/zyxin	Outside–in	2 and 24	Decreased total and mature FA, reduced ECM degradation [159]
AuNP	Human umbilical vein endothelial cells (HUVECs)	F-actin/vinculin	Inside–out	24	Reduced FA size and impaired F-actin and tubulin polymerization [155]
SiO ₂	Oral mucosa cells TR156	F-actin/vinculin	Inside–out	12	Increased F-actin filament traction, increased FA formation Decreased cell migration [161]
TiO ₂	Oral mucosa cells TR156	F-actin/vinculin	Inside–out	12	Increased F-actin filament traction, increased FA formation Decreased cell migration [161]
Hydroxyapatite	Oral mucosa cells TR156	F-actin/vinculin	Inside–out	12	Increased F-actin filament traction, increased FA formation Decreased cell migration [161]
TiO ₂	Human osteoblast-like cells SaOS-2	F-actin/p-FAK	Inside–out	24	Decreased FA area, reduced cell migration Reduced vinculin [167]
Polyethylenimine@IONP	HUVEC	F-actin/vinculin p-cortactin	Inside–out	6	Lower phospho-cortactin ⁺ FA, reduced cell migration Reduced phospho-Src and phospho-cortactin ROS involvement [154]

The disturbance mentioned above of cytoskeleton dynamics upon inorganic nanoparticle uptake translates into a global mechanical change at the cellular level, recently demonstrated by Perez, J.E. et al. [170]. Measuring the deformation of a single mouse embryonal carcinoma F9 cell ($d(t)$), caught between two glass plates, one rigid and another flexible, Perez, J.E. et al. recorded a transient increase in cell viscoelastic module (G) after treatment with citrate-coated γ -Fe₂O₃ nanoparticles. This behavior indicated an increment in cell stiffness, most likely related to the rise in the stress fiber density in the first 30 min after nanoparticle treatment.

The studies above relied on nanoparticle internalization (inside–out). However, nanoparticles can impart changes to cytoskeleton dynamics in an outside–in manner. Indeed, Lipski, A.M. et al. analyzed the impact of crystal roughness on bovine aortic

endothelial cells (BAECs) and mouse calvarial preosteoblasts (MC3T3-E1) coated crystal with 50–300 nm SiO₂ NP. Consequently, whereas the nanoparticle layer reduced FA size in BAECs, an increase in FA size was observed in MC3T3-E1, revealing a cell type bias [169], as demonstrated by others [155]. AuNP layers also impart cytoskeleton changes to mouse embryonic stem cells (mESCs) whereby smooth Au, nanorough AuNP surface (106 nm), and sub-microrough AuNP surface (<393 nm) appear to promote FA formation although with distinguishably distribution, i.e., in smooth Au mESCs display FAs mainly in the periphery while exhibiting a more random distribution in nanorough and sub-microrough AuNP layers [171]. On the contrary, mESCs cultured on microrough AuNP layers (>573 nm) display significantly fewer FAs as measured by vinculin expression, all suggesting that metallic surface typology can also modulate FA dynamics in an outside-in manner, as demonstrated by others [172–175]. The latter has consequences for biomaterial-based tissue engineering as the maintenance of the proper formation of FA in mESCs on smooth Au, nanorough, and sub-microrough AuNP layers, also correlated with the maintenance of cell pluripotency. In contrast, the low FA formation rate on microrough surfaces is conducive to osteoinduction [171,176].

3.2. Nanopaterneting as a Platform for FA Study

The extracellular pattern can modulate FA dynamics and ultimately shapes cellular topography. And here, metallic nanoparticles provide an invaluable tool to study adhesive structures under a controlled spatial patterning. Posa, F. et al. unraveled the synergistic effect of integrins and a bone morphogenic protein (BMP-2) in regulating FA size and clustering using a nanopatterned surface built by 50 nm-separated BMP-2-coated AuNPs and co-presented with integrin ligands [177]. Furthermore, the nanoparticle-based ECM nanopatterning can also furnish researchers with a remote-control system for cellular adhesion modulation. Representative work by Kang, H. et al. showed an integrin ligand (RGD) coupled to IONPs and attached to a glass surface by a flexible polyethylene glycol linker, that upon the application of an external oscillating magnetic field can either promote FA assembly or disassembly in human mesenchymal stem cells depending on the frequency of the magnetic field [178]. As such, when a slow magnetic field (0.1 Hz) is applied, oscillating IONPs promote RGD–integrin ligation and the formation and maturation of FAs both in vitro and in vivo. By contrast, a relatively faster magnetic field (2 Hz) inhibits FA formation and hampers RGD–integrin ligation. Curiously, either effect reversed when the magnetic field frequency was changed, demonstrating the remote-control capability of the system. Similar results were obtained by designing a strategy where an AuNP bridged the glass surface with a magnetic nanocage, and the RGD ligand was linked to the AuNP [179].

In addition to the potential of nanopatterned surfaces for study adhesome dynamics, colloidal inorganic nanoparticles have also proved helpful in deciphering structural features of adhesions. Recently, Okada, T. et al. developed a novel imaging microscopy technology named scanning electron-assisted dielectric-impedance microscopy (SE-ADM). Based on 60-nm colloidal gold nanoparticles coated with an integrin β 1-specific antibody, Okada, T. et al. showed that the adhesion core contains three or four integrin β 1-rich regions connected to actin bundles [180]. The importance of the techniques lies in the direct visualization of the living cells without staining or fixation.

3.3. Inorganic Nanoparticles and Invadosome Dynamic

The effects of inorganic nanoparticles on podosomes have been described primarily on cells of the mononuclear system, where these structures play a crucial role in cell migration and invasion. Mulens-Arias, V. et al. found that AuNP can promote podosome assembly into rosettes in the murine macrophage RAW 264.7, measured as phospho-cortactin-rich F-actin spots [159]. Such an increase in podosome rosette overlapped with an increment in podosome assembly and an exacerbated ECM degradation. However, there was a clear dependence on AuNP size, as the effects mentioned above were only observed for smaller nanoparticles <16 nm.

Very often, macrophages exhibiting a reduced migratory rate upon inorganic nanoparticle treatment show an increase in podosome-mediated ECM degradation. Rojas, J.M. et al. demonstrated that superparamagnetic iron oxide nanoparticles (SPION) coated with dimethyl succinic acid, 3-aminopropyl-triethoxysilane, or aminodextran, promoted podosome assembly in bone marrow-derived macrophages M2 and, thereby, an increment in ECM degradation while inhibited macrophage migration [181]. The latter can be explained by the consistent production of active MT1-MMP metalloproteinase upon SPION uptake by macrophages. Notably, the above effects on macrophage invasion behavior coincided with a global change in the activation profile, where important cytokines and chemokines were upregulated, such as *Tnfa*, *Il23a*, *Ccl2* mRNA, and critical signaling pathways activated, including the MAPK and AKT. Altogether, the SPION-induced podosome formations appeared to be associated with a macrophage activation mechanism rather than a direct effect.

Another study shed more evidence on the modulation of podosome dynamics as part of the macrophage activation process. Mulens-Arias, V. et al. found that the murine macrophage RAW 264.7 exhibited an activation shift toward an M1 phenotype when treated with two different PEI@MNP, as determined by the increment in activation markers CD80, CD83, CD40, and I-A/I-E, and the upregulation of several pro-immunogenic cytokine/chemokines, e.g., *Tnfa*, *Il1b*, *Arg1*, and *Ccl2* [182]. However, the exciting outcome for the interest of this review is the concomitant increase of podosome density, indicating that podosome dynamic shifts as macrophage activation status does. Contrarily to SPION effects on M2 macrophages, the rise in podosome density did not translate into an exacerbated ECM degradation; on the contrary, PEI@MNP-treated macrophages exhibited a reduced ECM degradation ability [182]. The first suspects behind such effects are the atomic iron and ROS, all products of the MNP intracellular degradation. The intracellular trafficking of MNP leads to NP degradation and, thus, the enrichment of the labile iron pool (LIP). The LIP contributes to the intracellular ROS level through the Fenton reaction, where the Fe^{2+} is converted into Fe^{3+} by H_2O_2 , producing hydroxyl radicals [183]. The excess of ROS acts as intermediates in several signaling pathways [184] and can promote podosome formation [71].

In another example of the influence of nanoparticles, cell activation, and podosome dynamics, Xu, J. et al. interrogated the impact of atomic cobalt (Co^{2+}) and cobalt nanoparticles (CoNPs) on macrophages to better understand the macrophage retention at the site of metallic implant, leading to the adverse retention to metal debris (ARMD) events [185]. When the U937 macrophages were treated with Co^{2+} or CoNPs, the researchers observed a profound inhibition of cell migration in vitro and in vivo. This effect was simultaneous with the hyper-acetylation of α -tubulin, leading to a global microtubule network rearrangement. As a result, macrophages showed increased cell spreading, adhesion, and podosome density. This increment in podosome density promoted an exacerbated ECM erosion, most likely due to the activation of the metalloproteinase MMP9. Notably, Xu, J. et al. demonstrated that Co^{2+} and CoNP effect on podosome formation is associated with ROS production that inhibits the activation of the Rho GTPase RhoA, a well-known regulator of actin and podosome turnover [186].

Like podosomes, invadopodia can also be affected by inorganic nanoparticle treatment due to a global cellular signaling shift. The murine pancreatic tumor adenocarcinoma cells, Pan 02, showed a reduced migratory rate and a diminished degradation of the collagen type IV-rich basement membrane upon treatment with PEI@MNPs [187]. When Mulens-Arias, V. et al. assessed the invadosome density, they found that the formation of invadosome in PEI@MNP-treated Pan 02 cells was severely hampered, most likely associated with reduced activation of the Src kinase. Notably, the reduction in invadosome density was accompanied by a downmodulation of metalloproteinases MT1-MMP and MMP2 and the upregulation of SerpinE1, a natural inhibitor of extracellular proteases [188]. Since SerpinE1 directly affects the protease activity and the cytoskeletal rearrangement and focal

adhesions, it is plausible that PEI@MNP-induced SerpinE1 limits extracellular protease activity and cell motility through the modulation of Jak/STAT1 signaling axis [189].

Altogether, inorganic nanoparticles can impart a global change in the intracellular signaling network that eventually leads to a profound shift in invadosome dynamics. Several intermediates have been described to drive such effects, including the production of reactive oxygen species, atomic metal such as iron, nanoparticle coating-induced cell membrane receptor activation, or direct interference with actin polymerization. Therefore, each new inorganic nanoparticle intended to be used as a theranostic agent should be thoroughly studied to evaluate any possible impact on adhesome dynamics that can hamper the final therapeutic goal or even enhance it.

4. Perspectives

Whether directly or indirectly, the influence of inorganic nanoparticles on cellular mechanical dynamics emerges as a potential therapeutic approach for diverse diseases such as cancer and tissue regeneration. The recent findings on nanoparticle-driven changes in adhesome dynamics and the increasing interest in dissecting the molecular mechanisms involved can accelerate the designing and exploitation of nanotheranostics for impairing or triggering cell migration as a basis for a therapeutic effect. For instance, the application of nanotheranostics to inhibit invadosome formation and, thus, ECM degradation might preclude primary tumor cells from invading surrounding healthy tissues and metastasize to other organs. However, a thorough analysis has to be made to elucidate the exact molecular mechanisms through which the nanoparticles inhibit such processes, knowing that each type of nanoparticle can behave differently. Thus, systematic research has to be performed regarding nanoparticle-driven adhesome changes as it is done for nanoparticle toxicity.

Notably, nanoparticles still cope with several drawbacks while reaching the clinical stage. Three well-defined levels of obstacles can be observed: (1) the pharmaceutical design, where the development of large-scale production under the good manufacturing practices standard and the quality control assays remain an essential obstacle; (2) the preclinical study, including pharmacokinetic and pharmacodynamics, where more precise and reproducible assays to detect early toxic effects in cells are needed, and a better understanding of the nanoparticle-cell (tissue) interaction is vital; and (3) the clinical stage, where there is still a limited regulatory guideline and a poor understanding of the nanoparticle biological interaction including the targeted site within the patient body. In this context, the interference of adhesome dynamics driven by nanoparticles and their comprehension can help overcome some of the obstacles identified in the preclinical and the clinical stages. At least, the study of adhesome dynamics must be considered paramount for elucidating the nanoparticle biological interaction with cells and biological tissues and, thus, pave its route toward the clinical stage. However, as it can be observed from this review, different biological and physical assays have been followed to study nanoparticle interference in adhesome dynamics, making it difficult to find points of comparison among nanoparticles. Therefore, researchers should also meet standardized protocols to dissect nanoparticle effects on adhesome dynamics to make results comparable and reproducible and facilitate nanoparticle translation to the clinic.

From the present review, it is clear that some inorganic nanoparticles are endowed with the intrinsic capacity to modulate adhesome dynamics and that such effects can be the basis for a therapeutic strategy. Furthermore, nanoparticle features traditionally known to influence their cell toxicity, internalization, and therapeutic outcome, also appear to affect nanoparticle-driven interference in adhesome dynamics. Like the AuNP size influence in FA dynamics, nanoparticle surface charge and protein corona might also determine the extent of the adhesome dynamic interference. Thus, future studies should address the impact of various nanoparticle properties (e.g., size, charge, protein corona, aggregation state, and intracellular degradation rate) to comprehend nanoparticle potentials fully. More importantly, these parameters also affect nanoparticle biodistribution and, thus, link nanoparticle behavior in vivo to the local effects.

To exploit nanoparticles as adhesome modulators, researchers must overcome the traditional hurdles for nanotheranostics, i.e., tissue specificity, biodistribution, pharmacodynamics, and systemic toxicity. Besides, the nanoparticle can be modified to increase tissue specificity or longer circulation time and impart signal input to the cytoskeleton network to change cell migration/invasion. Among them, the use of integrin ligands or agonists and kinase inhibitors as cargo might provide potential use.

Funding: This review received no external funding.

Conflicts of Interest: The author declares no conflict of interest.

References

- Habibi, N.; Quevedo, D.F.; Gregory, J.V.; Lahann, J. Emerging Methods in Therapeutics Using Multifunctional Nanoparticles. *WIREs Nanomed. Nanobiotechnol.* **2020**, *12*, e1625. [\[CrossRef\]](#) [\[PubMed\]](#)
- Khan, A.U.; Khan, M.; Cho, M.H.; Khan, M.M. Selected Nanotechnologies and Nanostructures for Drug Delivery, Nanomedicine and Cure. *Bioprocess Biosyst. Eng.* **2020**, *43*, 1339–1357. [\[CrossRef\]](#)
- Wicki, A.; Witzigmann, D.; Balasubramanian, V.; Huwyler, J. Nanomedicine in Cancer Therapy: Challenges, Opportunities, and Clinical Applications. *J. Control. Release* **2015**, *200*, 138–157. [\[CrossRef\]](#)
- Hare, J.I.; Lammers, T.; Ashford, M.B.; Puri, S.; Storm, G.; Barry, S.T. Challenges and Strategies in Anti-Cancer Nanomedicine Development: An Industry Perspective. *Adv. Drug Deliv. Rev.* **2017**, *108*, 25–38. [\[CrossRef\]](#)
- Gharagozloo, M.; Majewski, S.; Foldvari, M. Therapeutic Applications of Nanomedicine in Autoimmune Diseases: From Immunosuppression to Tolerance Induction. *Nanomed. Nanotechnol. Biol. Med.* **2015**, *11*, 1003–1018. [\[CrossRef\]](#)
- Qamar, N.; Arif, A.; Bhatti, A.; John, P. Nanomedicine: An Emerging Era of Theranostics and Therapeutics for Rheumatoid Arthritis. *Rheumatology* **2019**, *58*, 1715–1721. [\[CrossRef\]](#) [\[PubMed\]](#)
- Poovaliah, N.; Davoudi, Z.; Peng, H.; Schlichtmann, B.; Mallapragada, S.; Narasimhan, B.; Wang, Q. Treatment of Neurodegenerative Disorders through the Blood–Brain Barrier Using Nanocarriers. *Nanoscale* **2018**, *10*, 16962–16983. [\[CrossRef\]](#)
- Ramanathan, S.; Archunan, G.; Sivakumar, M.; Selvan, S.T.; Fred, A.L.; Kumar, S.; Gulyás, B.; Padmanabhan, P. Theranostic Applications of Nanoparticles in Neurodegenerative Disorders. *Int. J. Nanomed.* **2018**, *13*, 5561–5576. [\[CrossRef\]](#)
- Steichen, S.D.; Caldorera-Moore, M.; Peppas, N.A. A Review of Current Nanoparticle and Targeting Moieties for the Delivery of Cancer Therapeutics. *Eur. J. Pharm. Sci.* **2013**, *48*, 416–427. [\[CrossRef\]](#) [\[PubMed\]](#)
- Amreddy, N.; Babu, A.; Muralidharan, R.; Panneerselvam, J.; Srivastava, A.; Ahmed, R.; Mehta, M.; Munshi, A.; Ramesh, R. Chapter Five—Recent Advances in Nanoparticle-Based Cancer Drug and Gene Delivery. In *Advances in Cancer Research*; Tew, K.D., Fisher, P.B., Eds.; Academic Press: Cambridge, MA, USA, 2018; Volume 137, pp. 115–170. ISBN 0065-230X.
- Deirram, N.; Zhang, C.; Keremian, S.S.; Johnston, A.P.R.; Such, G.K. PH-Responsive Polymer Nanoparticles for Drug Delivery. *Macromol. Rapid Commun.* **2019**, *40*, 1800917. [\[CrossRef\]](#) [\[PubMed\]](#)
- Karimi, M.; Eslami, M.; Sahandi-Zangabad, P.; Mirab, F.; Farajisafiloo, N.; Shafaei, Z.; Ghosh, D.; Bozorgomid, M.; Dashkhaneh, F.; Hamblin, M.R. PH-Sensitive Stimulus-Responsive Nanocarriers for Targeted Delivery of Therapeutic Agents. *WIREs Nanomed. Nanobiotechnol.* **2016**, *8*, 696–716. [\[CrossRef\]](#) [\[PubMed\]](#)
- Xu, X.; Saw, P.E.; Tao, W.; Li, Y.; Ji, X.; Bhasin, S.; Liu, Y.; Ayyash, D.; Rasmussen, J.; Huo, M.; et al. ROS-Responsive Polyprodrug Nanoparticles for Triggered Drug Delivery and Effective Cancer Therapy. *Adv. Mater.* **2017**, *29*, 1700141. [\[CrossRef\]](#)
- Lv, X.; Zhu, Y.; Ghandehari, H.; Yu, A.; Wang, Y. An ROS-Responsive and Self-Accelerating Drug Release Nanoplatfor for Overcoming Multidrug Resistance. *Chem. Commun.* **2019**, *55*, 3383–3386. [\[CrossRef\]](#) [\[PubMed\]](#)
- Halappanavar, S.; Vogel, U.; Wallin, H.; Yauk, C.L. Promise and Peril in Nanomedicine: The Challenges and Needs for Integrated Systems Biology Approaches to Define Health Risk. *WIREs Nanomed. Nanobiotechnol.* **2018**, *10*, e1465. [\[CrossRef\]](#) [\[PubMed\]](#)
- Pelaz, B.; Charron, G.; Pfeiffer, C.; Zhao, Y.; de la Fuente, J.M.; Liang, X.-J.; Parak, W.J.; Del Pino, P. Interfacing Engineered Nanoparticles with Biological Systems: Anticipating Adverse Nano-Bio Interactions. *Small* **2013**, *9*, 1573–1584. [\[CrossRef\]](#)
- Su, H.; Wang, Y.; Gu, Y.; Bowman, L.; Zhao, J.; Ding, M. Potential Applications and Human Biosafety of Nanomaterials Used in Nanomedicine. *J. Appl. Toxicol.* **2018**, *38*, 3–24. [\[CrossRef\]](#)
- Tang, D.D.; Gerlach, B.D. The Roles and Regulation of the Actin Cytoskeleton, Intermediate Filaments and Microtubules in Smooth Muscle Cell Migration. *Respir. Res.* **2017**, *18*, 54. [\[CrossRef\]](#)
- Fife, C.M.; McCarroll, J.A.; Kavallaris, M. Movers and Shakers: Cell Cytoskeleton in Cancer Metastasis. *Br. J. Pharmacol.* **2014**, *171*, 5507–5523. [\[CrossRef\]](#) [\[PubMed\]](#)
- Burbage, M.; Keppler, S.J. Shaping the Humoral Immune Response: Actin Regulators Modulate Antigen Presentation and Influence B-T Interactions. *Mol. Immunol.* **2018**, *101*, 370–376. [\[CrossRef\]](#) [\[PubMed\]](#)
- Mostowy, S.; Shenoy, A.R. The Cytoskeleton in Cell-Autonomous Immunity: Structural Determinants of Host Defence. *Nat. Rev. Immunol.* **2015**, *15*, 559–573. [\[CrossRef\]](#)
- Nishimura, Y.; Kasahara, K.; Inagaki, M. Intermediate Filaments and IF-Associated Proteins: From Cell Architecture to Cell Proliferation. *Proc. Jpn. Acad. Ser. B Phys. Biol. Sci.* **2019**, *95*, 479–493. [\[CrossRef\]](#)

23. Pawlik, A.; Szczepanski, M.A.; Klimaszewska-Wisniewska, A.; Gackowska, L.; Zuryn, A.; Grzanka, A. Cytoskeletal Reorganization and Cell Death in Mitoxantrone-Treated Lung Cancer Cells. *Acta Histochem.* **2016**, *118*, 784–796. [[CrossRef](#)]
24. Zaidel-Bar, R.; Itzkovitz, S.; Ma'ayan, A.; Iyengar, R.; Geiger, B. Functional Atlas of the Integrin Adhesome. *Nat. Cell Biol.* **2007**, *9*, 858–867. [[CrossRef](#)]
25. Winograd-Katz, S.E.; Fässler, R.; Geiger, B.; Legate, K.R. The Integrin Adhesome: From Genes and Proteins to Human Disease. *Nat. Rev. Mol. Cell Biol.* **2014**, *15*, 273–288. [[CrossRef](#)]
26. Singer, I.I.; Scott, S.; Kawka, D.W.; Kazazis, D.M. Adhesomes: Specific Granules Containing Receptors for Laminin, C3bi/Fibrinogen, Fibronectin, and Vitronectin in Human Polymorphonuclear Leukocytes and Monocytes. *J. Cell Biol.* **1989**, *109*, 3169–3182. [[CrossRef](#)] [[PubMed](#)]
27. Whittaker, C.A.; Bergeron, K.-F.; Whittle, J.; Brandhorst, B.P.; Burke, R.D.; Hynes, R.O. The Echinoderm Adhesome. *Dev. Biol.* **2006**, *300*, 252–266. [[CrossRef](#)] [[PubMed](#)]
28. Jacquemet, G.; Hamidi, H.; Ivaska, J. Filopodia in Cell Adhesion, 3D Migration and Cancer Cell Invasion. *Curr. Opin. Cell Biol.* **2015**, *36*, 23–31. [[CrossRef](#)] [[PubMed](#)]
29. Innocenti, M. New Insights into the Formation and the Function of Lamellipodia and Ruffles in Mesenchymal Cell Migration. *Cell Adhes. Migr.* **2018**, *12*, 401–416. [[CrossRef](#)] [[PubMed](#)]
30. Burridge, K.; Guilluy, C. Focal Adhesions, Stress Fibers and Mechanical Tension. *Exp. Cell Res.* **2016**, *343*, 14–20. [[CrossRef](#)]
31. Alonso, F.; Spuul, P.; Daubon, T.; Kramer, I.; Génot, E. Variations on the Theme of Podosomes: A Matter of Context. *Biochim. Biophys. Acta Mol. Cell Res.* **2019**, *1866*, 545–553. [[CrossRef](#)] [[PubMed](#)]
32. Cmoch, A.; Groves, P.; Piśula, S. Biogenesis of Invadopodia and Their Cellular Functions. *Postepy Biochem.* **2014**, *60*, 62–68.
33. Phng, L.-K.; Gebala, V.; Bentley, K.; Philippides, A.; Wacker, A.; Mathivet, T.; Sauter, L.; Stanchi, F.; Belting, H.-G.; Affolter, M.; et al. Formin-Mediated Actin Polymerization at Endothelial Junctions Is Required for Vessel Lumen Formation and Stabilization. *Dev. Cell* **2015**, *32*, 123–132. [[CrossRef](#)] [[PubMed](#)]
34. Sahasrabudhe, A.; Ghatge, K.; Mutalik, S.; Jacob, A.; Ghose, A. Formin 2 Regulates the Stabilization of Filopodial Tip Adhesions in Growth Cones and Affects Neuronal Outgrowth and Pathfinding In Vivo. *Development* **2016**, *143*, 449–460. [[CrossRef](#)] [[PubMed](#)]
35. Grobe, H.; Wüstenhagen, A.; Baarlink, C.; Grosse, R.; Grikscheit, K. A Rac1-FMN2 Signaling Module Affects Cell-Cell Contact Formation Independent of Cdc42 and Membrane Protrusions. *PLoS ONE* **2018**, *13*, e0194716. [[CrossRef](#)] [[PubMed](#)]
36. Disanza, A.; Bisi, S.; Winterhoff, M.; Milanesi, F.; Ushakov, D.S.; Kast, D.; Marighetti, P.; Romet-Lemonne, G.; Müller, H.-M.; Nickel, W.; et al. CDC42 Switches IRSp53 from Inhibition of Actin Growth to Elongation by Clustering of VASP. *EMBO J.* **2013**, *32*, 2735–2750. [[CrossRef](#)]
37. Chacón, M.R.; Navarro, A.I.; Cuesto, G.; del Pino, I.; Scott, R.; Morales, M.; Rico, B. Focal Adhesion Kinase Regulates Actin Nucleation and Neuronal Filopodia Formation during Axonal Growth. *Development* **2012**, *139*, 3200–3210. [[CrossRef](#)]
38. Young, L.E.; Latario, C.J.; Higgs, H.N. Roles for Ena/VASP Proteins in FMNL3-Mediated Filopodial Assembly. *J. Cell Sci.* **2018**, *131*, jcs220814. [[CrossRef](#)] [[PubMed](#)]
39. Barzik, M.; McClain, L.M.; Gupton, S.L.; Gertler, F.B. Ena/VASP Regulates MDIA2-Initiated Filopodial Length, Dynamics, and Function. *Mol. Biol. Cell* **2014**, *25*, 2604–2619. [[CrossRef](#)]
40. Alieva, N.O.; Efremov, A.K.; Hu, S.; Oh, D.; Chen, Z.; Natarajan, M.; Ong, H.T.; Jégou, A.; Romet-Lemonne, G.; Groves, J.T.; et al. Myosin IIA and Formin Dependent Mechanosensitivity of Filopodia Adhesion. *Nat. Commun.* **2019**, *10*, 3593. [[CrossRef](#)]
41. Hogg, N.; Laschinger, M.; Giles, K.; McDowall, A. T-Cell Integrins: More than Just Sticking Points. *J. Cell Sci.* **2003**, *116*, 4695–4705. [[CrossRef](#)]
42. Pröls, F.; Sagar, S.; Scaal, M. Signaling Filopodia in Vertebrate Embryonic Development. *Cell. Mol. Life Sci.* **2016**, *73*, 961–974. [[CrossRef](#)] [[PubMed](#)]
43. Romero, S.; Quatela, A.; Bornschlög, T.; Guadagnini, S.; Bassereau, P.; Van Nhieu, G.T. Filopodium Retraction Is Controlled by Adhesion to Its Tip. *J. Cell Sci.* **2012**, *125*, 4999–5004. [[CrossRef](#)]
44. Wong, S.; Guo, W.-H.; Wang, Y.-L. Fibroblasts Probe Substrate Rigidity with Filopodia Extensions before Occupying an Area. *Proc. Natl. Acad. Sci. USA* **2014**, *111*, 17176–17181. [[CrossRef](#)] [[PubMed](#)]
45. Spinardi, L.; Rietdorf, J.; Nitsch, L.; Bono, M.; Tacchetti, C.; Way, M.; Marchisio, P.C. A Dynamic Podosome-like Structure of Epithelial Cells. *Exp. Cell Res.* **2004**, *295*, 360–374. [[CrossRef](#)]
46. Wang, Y.; McNiven, M.A. Invasive Matrix Degradation at Focal Adhesions Occurs via Protease Recruitment by a FAK–P130Cas Complex. *J. Cell Biol.* **2012**, *196*, 375–385. [[CrossRef](#)] [[PubMed](#)]
47. Luxenburg, C.; Geblinger, D.; Klein, E.; Anderson, K.; Hanein, D.; Geiger, B.; Addadi, L. The Architecture of the Adhesive Apparatus of Cultured Osteoclasts: From Podosome Formation to Sealing Zone Assembly. *PLoS ONE* **2007**, *2*, e179. [[CrossRef](#)]
48. Sharma, V.P.; Eddy, R.; Entenberg, D.; Kai, M.; Gertler, F.B.; Condeelis, J. Tks5 and SHIP2 Regulate Invadopodium Maturation, but Not Initiation, in Breast Carcinoma Cells. *Curr. Biol.* **2013**, *23*, 2079–2089. [[CrossRef](#)]
49. Fu, P.; Ebenezer, D.L.; Berdyshev, E.V.; Bronova, I.A.; Shaaya, M.; Harijith, A.; Natarajan, V. Role of Sphingosine Kinase 1 and S1P Transporter Spns2 in HGF-Mediated Lamellipodia Formation in Lung Endothelium. *J. Biol. Chem.* **2016**, *291*, 27187–27203. [[CrossRef](#)]
50. Usatyuk, P.V.; Fu, P.; Mohan, V.; Epshtein, Y.; Jacobson, J.R.; Gomez-Cambronero, J.; Wary, K.K.; Bindokas, V.; Dudek, S.M.; Salgia, R.; et al. Role of C-Met/Phosphatidylinositol 3-Kinase (PI3K)/Akt Signaling in Hepatocyte Growth Factor (HGF)-Mediated

- Lamellipodia Formation, Reactive Oxygen Species (ROS) Generation, and Motility of Lung Endothelial Cells. *J. Biol. Chem.* **2014**, *289*, 13476–13491. [[CrossRef](#)] [[PubMed](#)]
51. Buhrmann, C.; Yazdi, M.; Popper, B.; Kunnumakkara, A.B.; Aggarwal, B.B.; Shakibaei, M. Induction of the Epithelial-to-Mesenchymal Transition of Human Colorectal Cancer by Human TNF- β (Lymphotoxin) and Its Reversal by Resveratrol. *Nutrients* **2019**, *11*, 704. [[CrossRef](#)] [[PubMed](#)]
 52. Gazquez, E.; Watanabe, Y.; Broders-Bondon, F.; Paul-Gilloteaux, P.; Heysch, J.; Baral, V.; Bondurand, N.; Dufour, S. Endothelin-3 Stimulates Cell Adhesion and Cooperates with B1-Integrins during Enteric Nervous System Ontogenesis. *Sci. Rep.* **2016**, *6*, 37877. [[CrossRef](#)] [[PubMed](#)]
 53. Savin, V.J.; Sharma, M.; Zhou, J.; Gennochi, D.; Fields, T.; Sharma, R.; McCarthy, E.T.; Srivastava, T.; Domen, J.; Tormo, A.; et al. Renal and Hematological Effects of CLCF-1, a B-Cell-Stimulating Cytokine of the IL-6 Family. *J. Immunol. Res.* **2015**, *2015*, 714964. [[CrossRef](#)] [[PubMed](#)]
 54. Kiso, M.; Tanaka, S.; Saji, S.; Toi, M.; Sato, F. Long Isoform of VEGF Stimulates Cell Migration of Breast Cancer by Filopodia Formation via NRP1/ARHGAP17/Cdc42 Regulatory Network. *Int. J. Cancer* **2018**, *143*, 2905–2918. [[CrossRef](#)]
 55. Feng, H.; Chen, L.; Wang, Q.; Shen, B.; Liu, L.; Zheng, P.; Xu, S.; Liu, X.; Chen, J.; Teng, J. Calumenin-15 Facilitates Filopodia Formation by Promoting TGF- β Superfamily Cytokine GDF-15 Transcription. *Cell Death Dis.* **2013**, *4*, e870. [[CrossRef](#)]
 56. Maisel, S.; Broka, D.; Schroeder, J. Intravascular Epidermal Growth Factor Receptor Subject to Retrograde Trafficking Drives Epidermal Growth Factor-Dependent Migration. *Oncotarget* **2017**, *9*, 6463–6477. [[CrossRef](#)]
 57. Shi, M.-D.; Liao, Y.-C.; Shih, Y.-W.; Tsai, L.-Y. Nobiletin Attenuates Metastasis via Both ERK and PI3K/Akt Pathways in HGF-Treated Liver Cancer HepG2 Cells. *Phytomedicine* **2013**, *20*, 743–752. [[CrossRef](#)]
 58. Marivin, A.; Berthelet, J.; Cartier, J.; Paul, C.; Gemble, S.; Morizot, A.; Boireau, W.; Saleh, M.; Bertoglio, J.; Solary, E.; et al. CIAP1 Regulates TNF-Mediated Cdc42 Activation and Filopodia Formation. *Oncogene* **2014**, *33*, 5534–5545. [[CrossRef](#)] [[PubMed](#)]
 59. Oswald, J.; Büttner, M.; Jasinski-Bergner, S.; Jacobs, R.; Rosenstock, P.; Kielstein, H. Leptin Affects Filopodia and Cofilin in NK-92 Cells in a Dose- and Time-Dependent Manner. *Eur. J. Histochem.* **2018**, *62*, 2848. [[CrossRef](#)] [[PubMed](#)]
 60. Rigracciolo, D.C.; Santolla, M.F.; Lappano, R.; Vivacqua, A.; Cirillo, F.; Galli, G.R.; Talia, M.; Muglia, L.; Pellegrino, M.; Nohata, N.; et al. Focal Adhesion Kinase (FAK) Activation by Estrogens Involves GPER in Triple-Negative Breast Cancer Cells. *J. Exp. Clin. Cancer Res.* **2019**, *38*, 58. [[CrossRef](#)]
 61. Nalluri, S.M.; O'Connor, J.W.; Virgi, G.A.; Stewart, S.E.; Ye, D.; Gomez, E.W. TGF β 1-Induced Expression of Caldesmon Mediates Epithelial–Mesenchymal Transition. *Cytoskeleton* **2018**, *75*, 201–212. [[CrossRef](#)]
 62. Johansson, M.W.; Khanna, M.; Bortnov, V.; Annis, D.S.; Nguyen, C.L.; Mosher, D.F. IL-5-Stimulated Eosinophils Adherent to Periostin Undergo Stereotypic Morphological Changes and ADAM8-Dependent Migration. *Clin. Exp. Allergy* **2017**, *47*, 1263–1274. [[CrossRef](#)]
 63. Daubon, T.; Spuul, P.; Alonso, F.; Fremaux, I.; Génot, E. VEGF-A Stimulates Podosome-Mediated Collagen-IV Proteolysis in Microvascular Endothelial Cells. *J. Cell Sci.* **2016**, *129*, 2586–2598. [[CrossRef](#)]
 64. Williams, K.S.; Killebrew, D.A.; Clary, G.P.; Seawell, J.A.; Meeker, R.B. Differential Regulation of Macrophage Phenotype by Mature and Pro-Nerve Growth Factor. *J. Neuroimmunol.* **2015**, *285*, 76–93. [[CrossRef](#)] [[PubMed](#)]
 65. Serafino, A.; Andreola, F.; Pittaluga, E.; Krasnowska, E.K.; Nicotera, G.; Sferrazza, G.; Sinibaldi Vallebbona, P.; Pierimarchi, P.; Garaci, E. Thymosin A1 Modifies Podosome Architecture and Promptly Stimulates the Expression of Podosomal Markers in Mature Macrophages. *Expert Opin. Biol. Ther.* **2015**, *15*, 101–116. [[CrossRef](#)] [[PubMed](#)]
 66. Kung, M.-L.; Tsai, H.-E.; Hu, T.-H.; Kuo, H.-M.; Liu, L.-F.; Chen, S.-C.; Lin, P.-R.; Ma, Y.-L.; Wang, E.-M.; Liu, G.-S.; et al. Hepatoma-Derived Growth Factor Stimulates Podosome Rosettes Formation in NIH/3T3 Cells through the Activation of Phosphatidylinositol 3-Kinase/Akt Pathway. *Biochem. Biophys. Res. Commun.* **2012**, *425*, 169–176. [[CrossRef](#)] [[PubMed](#)]
 67. Le Roux-Goglin, E.; Varon, C.; Spuul, P.; Asencio, C.; Mégraud, F.; Génot, E. Helicobacter Infection Induces Podosome Assembly in Primary Hepatocytes In Vitro. *Eur. J. Cell Biol.* **2012**, *91*, 161–170. [[CrossRef](#)]
 68. Tatin, F.; Grise, F.; Reuzeau, E.; Genot, E.; Moreau, V. Sodium Fluoride Induces Podosome Formation in Endothelial Cells. *Biol. Cell* **2010**, *102*, 489–498. [[CrossRef](#)] [[PubMed](#)]
 69. Sa, G.; Liu, Z.; Ren, J.; Wan, Q.; Xiong, X.; Yu, Z.; Chen, H.; Zhao, Y.; He, S. Keratinocyte Growth Factor (KGF) Induces Podosome Formation via Integrin-Erk1/2 Signaling in Human Immortalized Oral Epithelial Cells. *Cell. Signal.* **2019**, *61*, 39–47. [[CrossRef](#)]
 70. Griera, M.; Martin-Villar, E.; Banon-Rodríguez, I.; Blundell, M.P.; Jones, G.E.; Anton, I.M.; Thrasher, A.J.; Rodríguez-Puyol, M.; Calle, Y. Integrin Linked Kinase (ILK) Regulates Podosome Maturation and Stability in Dendritic Cells. *Int. J. Biochem. Cell Biol.* **2014**, *50*, 47–54. [[CrossRef](#)]
 71. Mu, X.; Wang, X.; Huang, W.; Wang, R.-T.; Essandoh, K.; Li, Y.; Pugh, A.M.; Peng, J.; Deng, S.; Wang, Y.; et al. Circulating Exosomes Isolated from Septic Mice Induce Cardiovascular Hyperpermeability Through Promoting Podosome Cluster Formation. *Shock* **2018**, *49*, 429–441. [[CrossRef](#)]
 72. Singh, A.; Gill, G.; Kaur, H.; Amhmed, M.; Jakhu, H. Role of Osteopontin in Bone Remodeling and Orthodontic Tooth Movement: A Review. *Prog. Orthod.* **2018**, *19*, 18. [[CrossRef](#)]
 73. Mader, C.C.; Oser, M.; Magalhaes, M.A.O.; Bravo-Cordero, J.J.; Condeelis, J.; Koleske, A.J.; Gil-Henn, H. An EGFR–Src–Arg–Cortactin Pathway Mediates Functional Maturation of Invadopodia and Breast Cancer Cell Invasion. *Cancer Res.* **2011**, *71*, 1730–1741. [[CrossRef](#)] [[PubMed](#)]

74. Eckert, M.A.; Lwin, T.M.; Chang, A.T.; Kim, J.; Danis, E.; Ohno-Machado, L.; Yang, J. Twist1-Induced Invadopodia Formation Promotes Tumor Metastasis. *Cancer Cell* **2011**, *19*, 372–386. [\[CrossRef\]](#)
75. Pignatelli, J.; Tumbarello, D.A.; Schmidt, R.P.; Turner, C.E. Hic-5 Promotes Invadopodia Formation and Invasion during TGF- β -Induced Epithelial–Mesenchymal Transition. *J. Cell Biol.* **2012**, *197*, 421–437. [\[CrossRef\]](#) [\[PubMed\]](#)
76. Hoshino, D.; Branch, K.M.; Weaver, A.M. Signaling Inputs to Invadopodia and Podosomes. *J. Cell Sci.* **2013**, *126*, 2979–2989. [\[CrossRef\]](#)
77. Rajadurai, C.V.; Havrylov, S.; Zaoui, K.; Vaillancourt, R.; Stuiblé, M.; Naujokas, M.; Zuo, D.; Tremblay, M.L.; Park, M. Met Receptor Tyrosine Kinase Signals through a Cortactin–Gab1 Scaffold Complex, to Mediate Invadopodia. *J. Cell Sci.* **2012**, *125*, 2940–2953. [\[CrossRef\]](#)
78. Makowiecka, A.; Simiczyjew, A.; Nowak, D.; Mazur, A.J. Varying Effects of EGF, HGF and TGF β on Formation of Invadopodia and Invasiveness of Melanoma Cell Lines of Different Origin. *Eur. J. Histochem.* **2016**, *60*, 2728. [\[CrossRef\]](#) [\[PubMed\]](#)
79. Chen, L.; Zhu, M.; Yu, S.; Hai, L.; Zhang, L.; Zhang, C.; Zhao, P.; Zhou, H.; Wang, S.; Yang, X. Arg Kinase Mediates CXCL12/CXCR4-Induced Invadopodia Formation and Invasion of Glioma Cells. *Exp. Cell Res.* **2020**, *389*, 216–229. [\[CrossRef\]](#)
80. Love, A.M.; Prince, D.J.; Jessen, J.R. Vangl2-Dependent Regulation of Membrane Protrusions and Directed Migration Requires a Fibronectin Extracellular Matrix. *Development* **2018**, *145*, dev165472. [\[CrossRef\]](#) [\[PubMed\]](#)
81. Singh, R. Central Role of PI3K-SYK Interaction in Fibrinogen-Induced Lamellipodia and Filopodia Formation in Platelets. *FEBS Open Bio.* **2016**, *6*, 1285–1296. [\[CrossRef\]](#)
82. Wang, W.Y.; Pearson, A.T.; Kutys, M.L.; Choi, C.K.; Wozniak, M.A.; Baker, B.M.; Chen, C.S. Extracellular Matrix Alignment Dictates the Organization of Focal Adhesions and Directs Uniaxial Cell Migration. *APL Bioeng.* **2018**, *2*, 046107. [\[CrossRef\]](#) [\[PubMed\]](#)
83. Diaz, C.; Neubauer, S.; Rechenmacher, F.; Kessler, H.; Missirlis, D. Recruitment of $\alpha_v\beta_3$ Integrin to $\alpha_5\beta_1$ Integrin-Induced Clusters Enables Focal Adhesion Maturation and Cell Spreading. *J. Cell Sci.* **2020**, *133*, jcs232702. [\[CrossRef\]](#)
84. Stritt, S.; Thielmann, I.; Dütting, S.; Stegner, D.; Nieswandt, B. Phospholipase D Is a Central Regulator of Collagen I-Induced Cytoskeletal Rearrangement and Podosome Formation in Megakaryocytes. *J. Thromb. Haemost.* **2014**, *12*, 1364–1371. [\[CrossRef\]](#)
85. Schachtner, H.; Calaminus, S.D.J.; Sinclair, A.; Monypenny, J.; Blundell, M.P.; Leon, C.; Holyoake, T.L.; Thrasher, A.J.; Michie, A.M.; Vukovic, M.; et al. Megakaryocytes Assemble Podosomes That Degrade Matrix and Protrude through Basement Membrane. *Blood* **2013**, *121*, 2542–2552. [\[CrossRef\]](#) [\[PubMed\]](#)
86. Suzuki, T.; Shoji, S.; Yamamoto, K.; Nada, S.; Okada, M.; Yamamoto, T.; Honda, Z. Essential Roles of Lyn in Fibronectin-Mediated Filamentous Actin Assembly and Cell Motility in Mast Cells. *J. Immunol.* **1998**, *161*, 3694–3701. [\[PubMed\]](#)
87. Beaty, B.T.; Sharma, V.P.; Bravo-Cordero, J.J.; Simpson, M.A.; Eddy, R.J.; Koleske, A.J.; Condeelis, J. B1 Integrin Regulates Arg to Promote Invadopodial Maturation and Matrix Degradation. *MBoC* **2013**, *24*, 1661–1675. [\[CrossRef\]](#)
88. Artym, V.V.; Swatkoski, S.; Matsumoto, K.; Campbell, C.B.; Petrie, R.J.; Dimitriadis, E.K.; Li, X.; Mueller, S.C.; Bugge, T.H.; Gucuk, M.; et al. Dense Fibrillar Collagen Is a Potent Inducer of Invadopodia via a Specific Signaling Network. *J. Cell Biol.* **2015**, *208*, 331–350. [\[CrossRef\]](#)
89. Di Martino, J.; Moreau, V.; Saltel, F. Type I Collagen Fibrils: An Inducer of Invadosomes. *Oncotarget* **2015**, *6*, 28519–28520. [\[CrossRef\]](#) [\[PubMed\]](#)
90. Zhao, P.; Xu, Y.; Wei, Y.; Qiu, Q.; Chew, T.-L.; Kang, Y.; Cheng, C. The CD44s Splice Isoform Is a Central Mediator for Invadopodia Activity. *J. Cell Sci.* **2016**, *129*, 1355–1365. [\[CrossRef\]](#) [\[PubMed\]](#)
91. Burridge, K. Focal Adhesions: A Personal Perspective on a Half Century of Progress. *FEBS J.* **2017**, *284*, 3355–3361. [\[CrossRef\]](#) [\[PubMed\]](#)
92. Tai, Y.-L.; Chen, L.-C.; Shen, T.-L. Emerging Roles of Focal Adhesion Kinase in Cancer. *Biomed. Res. Int.* **2015**, *2015*, 690690. [\[CrossRef\]](#)
93. Tomakidi, P.; Schulz, S.; Proksch, S.; Weber, W.; Steinberg, T. Focal Adhesion Kinase (FAK) Perspectives in Mechanobiology: Implications for Cell Behaviour. *Cell Tissue Res.* **2014**, *357*, 515–526. [\[CrossRef\]](#)
94. Schlaepfer, D.D.; Mitra, S.K.; Ilic, D. Control of Motile and Invasive Cell Phenotypes by Focal Adhesion Kinase. *Biochim. Biophys. Acta Mol. Cell Res.* **2004**, *1692*, 77–102. [\[CrossRef\]](#)
95. Sarangi, B.R.; Gupta, M.; Doss, B.L.; Tissot, N.; Lam, F.; Mège, R.-M.; Borghi, N.; Ladoux, B. Coordination between Intra- and Extracellular Forces Regulates Focal Adhesion Dynamics. *Nano Lett.* **2017**, *17*, 399–406. [\[CrossRef\]](#) [\[PubMed\]](#)
96. Larsen, M.; Artym, V.V.; Green, J.A.; Yamada, K.M. The Matrix Reorganized: Extracellular Matrix Remodeling and Integrin Signaling. *Curr. Opin. Cell Biol.* **2006**, *18*, 463–471. [\[CrossRef\]](#)
97. Hu, Y.-L.; Lu, S.; Szeto, K.W.; Sun, J.; Wang, Y.; Lasheras, J.C.; Chien, S. FAK and Paxillin Dynamics at Focal Adhesions in the Protrusions of Migrating Cells. *Sci. Rep.* **2014**, *4*, 6024. [\[CrossRef\]](#) [\[PubMed\]](#)
98. Ciobanasu, C.; Faivre, B.; Le Clainche, C. Integrating Actin Dynamics, Mechanotransduction and Integrin Activation: The Multiple Functions of Actin Binding Proteins in Focal Adhesions. *Eur. J. Cell Biol.* **2013**, *92*, 339–348. [\[CrossRef\]](#)
99. Stutchbury, B.; Atherton, P.; Tsang, R.; Wang, D.-Y.; Ballestrem, C. Distinct Focal Adhesion Protein Modules Control Different Aspects of Mechanotransduction. *J. Cell Sci.* **2017**, *130*, 1612–1624. [\[CrossRef\]](#) [\[PubMed\]](#)
100. Zhou, D.W.; Lee, T.T.; Weng, S.; Fu, J.; García, A.J. Effects of Substrate Stiffness and Actomyosin Contractility on Coupling between Force Transmission and Vinculin–Paxillin Recruitment at Single Focal Adhesions. *Mol. Biol. Cell* **2017**, *28*, 1901–1911. [\[CrossRef\]](#)

101. Grashoff, C.; Hoffman, B.D.; Brenner, M.D.; Zhou, R.; Parsons, M.; Yang, M.T.; McLean, M.A.; Sligar, S.G.; Chen, C.S.; Ha, T.; et al. Measuring Mechanical Tension across Vinculin Reveals Regulation of Focal Adhesion Dynamics. *Nature* **2010**, *466*, 263–266. [[CrossRef](#)] [[PubMed](#)]
102. Atherton, P.; Stutchbury, B.; Wang, D.-Y.; Jethwa, D.; Tsang, R.; Meiler-Rodriguez, E.; Wang, P.; Bate, N.; Zent, R.; Barsukov, I.L.; et al. Vinculin Controls Talin Engagement with the Actomyosin Machinery. *Nat. Commun.* **2015**, *6*, 10038. [[CrossRef](#)] [[PubMed](#)]
103. Omachi, T.; Ichikawa, T.; Kimura, Y.; Ueda, K.; Kioka, N. Vinculin Association with Actin Cytoskeleton Is Necessary for Stiffness-Dependent Regulation of Vinculin Behavior. *PLoS ONE* **2017**, *12*, e0175324. [[CrossRef](#)]
104. Calderwood, D.A.; Campbell, I.D.; Critchley, D.R. Talins and Kindlins: Partners in Integrin-Mediated Adhesion. *Nat. Rev. Mol. Cell Biol.* **2013**, *14*, 503–517. [[CrossRef](#)] [[PubMed](#)]
105. Chan, Z.C.-K.; Kwan, H.-L.R.; Wong, Y.S.; Jiang, Z.; Zhou, Z.; Tam, K.W.; Chan, Y.-S.; Chan, C.B.; Lee, C.W. Site-Directed MT1-MMP Trafficking and Surface Insertion Regulate AChR Clustering and Remodeling at Developing NMJs. *eLife* **2020**, *9*, e54379. [[CrossRef](#)]
106. El Azzouzi, K.; Wiesner, C.; Linder, S. Metalloproteinase MT1-MMP Islets Act as Memory Devices for Podosome Reemergence. *J. Cell Biol.* **2016**, *213*, 109–125. [[CrossRef](#)] [[PubMed](#)]
107. Infante, E.; Castagnino, A.; Ferrari, R.; Monteiro, P.; Agüera-González, S.; Paul-Gilloteaux, P.; Domingues, M.J.; Maiuri, P.; Raab, M.; Shanahan, C.M.; et al. LINC Complex-Lis1 Interplay Controls MT1-MMP Matrix Digest-on-Demand Response for Confined Tumor Cell Migration. *Nat. Commun.* **2018**, *9*, 2443. [[CrossRef](#)]
108. Kuo, S.-L.; Chen, C.-L.; Pan, Y.-R.; Chiu, W.-T.; Chen, H.-C. Biogenesis of Podosome Rosettes through Fission. *Sci. Rep.* **2018**, *8*, 524. [[CrossRef](#)] [[PubMed](#)]
109. Van den Dries, K.; Schwartz, S.L.; Byars, J.; Meddens, M.B.M.; Bolomini-Vittori, M.; Lidke, D.S.; Figdor, C.G.; Lidke, K.A.; Cambi, A. Dual-Color Superresolution Microscopy Reveals Nanoscale Organization of Mechanosensory Podosomes. *Mol. Biol. Cell* **2013**, *24*, 2112–2123. [[CrossRef](#)]
110. Shattil, S.J.; O'Toole, T.; Eigenthaler, M.; Thon, V.; Williams, M.; Babior, B.M.; Ginsberg, M.H. Beta 3-Endonexin, a Novel Polypeptide That Interacts Specifically with the Cytoplasmic Tail of the Integrin Beta 3 Subunit. *J. Cell Biol.* **1995**, *131*, 807–816. [[CrossRef](#)] [[PubMed](#)]
111. Ray, R.M.; Li, C.; Bhattacharya, S.; Naren, A.P.; Johnson, L.R. Spermine, a Molecular Switch Regulating EGFR, Integrin B3, Src, and FAK Scaffolding. *Cell. Signal.* **2012**, *24*, 931–942. [[CrossRef](#)]
112. Proag, A.; Bouissou, A.; Mangeat, T.; Voituriez, R.; Delobelle, P.; Thibault, C.; Vieu, C.; Maridonneau-Parini, I.; Poincloux, R. Working Together: Spatial Synchrony in the Force and Actin Dynamics of Podosome First Neighbors. *ACS Nano* **2015**, *9*, 3800–3813. [[CrossRef](#)]
113. Bhuwania, R.; Cornfine, S.; Fang, Z.; Krüger, M.; Luna, E.J.; Linder, S. Supervillin Couples Myosin-Dependent Contractility to Podosomes and Enables Their Turnover. *J. Cell Sci.* **2012**, *125*, 2300–2314. [[CrossRef](#)] [[PubMed](#)]
114. Joosten, B.; Willemse, M.; Fransen, J.; Cambi, A.; van den Dries, K. Super-Resolution Correlative Light and Electron Microscopy (SR-CLEM) Reveals Novel Ultrastructural Insights Into Dendritic Cell Podosomes. *Front. Immunol.* **2018**, *9*, 1908. [[CrossRef](#)]
115. Cervero, P.; Wiesner, C.; Bouissou, A.; Poincloux, R.; Linder, S. Lymphocyte-Specific Protein 1 Regulates Mechanosensory Oscillation of Podosomes and Actin Isoform-Based Actomyosin Symmetry Breaking. *Nat. Commun.* **2018**, *9*, 515. [[CrossRef](#)] [[PubMed](#)]
116. Petropoulos, C.; Oddou, C.; Emadali, A.; Hiriart-Bryant, E.; Boyault, C.; Faurobert, E.; Vande Pol, S.; Kim-Kaneyama, J.-R.; Kraut, A.; Coute, Y.; et al. Roles of Paxillin Family Members in Adhesion and ECM Degradation Coupling at Invadosomes. *J. Cell Biol.* **2016**, *213*, 585–599. [[CrossRef](#)] [[PubMed](#)]
117. Walde, M.; Monypenny, J.; Heintzmann, R.; Jones, G.E.; Cox, S. Vinculin Binding Angle in Podosomes Revealed by High Resolution Microscopy. *PLoS ONE* **2014**, *9*, e88251. [[CrossRef](#)]
118. Praekelt, U.; Kopp, P.M.; Rehm, K.; Linder, S.; Bate, N.; Patel, B.; Debrand, E.; Manso, A.M.; Ross, R.S.; Conti, F.; et al. New Isoform-Specific Monoclonal Antibodies Reveal Different Sub-Cellular Localisations for Talin1 and Talin2. *Eur. J. Cell Biol.* **2012**, *91*, 180–191. [[CrossRef](#)]
119. Labernadie, A.; Thibault, C.; Vieu, C.; Maridonneau-Parini, I.; Charrière, G.M. Dynamics of Podosome Stiffness Revealed by Atomic Force Microscopy. *Proc. Natl. Acad. Sci. USA* **2010**, *107*, 21016–21021. [[CrossRef](#)]
120. Horton, M.A.; Nesbit, M.A.; Helfrich, M.H. Interaction of Osteopontin with Osteoclast Integrins. *Ann. N. Y. Acad. Sci.* **1995**, *760*, 190–200. [[CrossRef](#)]
121. Juin, A.; Billottet, C.; Moreau, V.; Destaing, O.; Albiges-Rizo, C.; Rosenbaum, J.; Génot, E.; Saltel, F. Physiological Type I Collagen Organization Induces the Formation of a Novel Class of Linear Invadosomes. *MBoC* **2011**, *23*, 297–309. [[CrossRef](#)]
122. Ferrari, R.; Infante, E.; Chavrier, P. Nucleus–Invadopodia Duo During Cancer Invasion. *Trends Cell Biol.* **2019**, *29*, 93–96. [[CrossRef](#)] [[PubMed](#)]
123. Castro-Castro, A.; Marchesin, V.; Monteiro, P.; Lodillinsky, C.; Rossé, C.; Chavrier, P. Cellular and Molecular Mechanisms of MT1-MMP-Dependent Cancer Cell Invasion. *Annu. Rev. Cell Dev. Biol.* **2016**, *32*, 555–576. [[CrossRef](#)]
124. Hastie, E.L.; Sherwood, D.R. A New Front in Cell Invasion: The Invadopodial Membrane. *Eur. J. Cell Biol.* **2016**, *95*, 441–448. [[CrossRef](#)] [[PubMed](#)]
125. Meirson, T.; Gil-Henn, H. Targeting Invadopodia for Blocking Breast Cancer Metastasis. *Drug Resist. Updates* **2018**, *39*, 1–17. [[CrossRef](#)] [[PubMed](#)]

126. Evans, J.G.; Correia, I.; Krasavina, O.; Watson, N.; Matsudaira, P. Macrophage Podosomes Assemble at the Leading Lamella by Growth and Fragmentation. *J. Cell Biol.* **2003**, *161*, 697–705. [[CrossRef](#)] [[PubMed](#)]
127. Calle, Y.; Chou, H.; Thrasher, A.J.; Jones, G.E. Wiskott–Aldrich Syndrome Protein and the Cytoskeletal Dynamics of Dendritic Cells. *J. Pathol.* **2004**, *204*, 460–469. [[CrossRef](#)]
128. Levy-Apter, E.; Finkelshtein, E.; Vemulapalli, V.; Li, S.S.-C.; Bedford, M.T.; Elson, A. Adaptor Protein GRB2 Promotes Src Tyrosine Kinase Activation and Podosomal Organization by Protein-Tyrosine Phosphatase ϵ in Osteoclasts. *J. Biol. Chem.* **2014**, *289*, 36048–36058. [[CrossRef](#)]
129. Tsuboi, S. Requirement for a Complex of Wiskott–Aldrich Syndrome Protein (WASP) with WASP Interacting Protein in Podosome Formation in Macrophages. *J. Immunol.* **2007**, *178*, 2987–2995. [[CrossRef](#)] [[PubMed](#)]
130. Pignatelli, J.; Bravo-Cordero, J.J.; Roh-Johnson, M.; Gandhi, S.J.; Wang, Y.; Chen, X.; Eddy, R.J.; Xue, A.; Singer, R.H.; Hodgson, L.; et al. Macrophage-Dependent Tumor Cell Transendothelial Migration Is Mediated by Notch1/MenaINV-Initiated Invadopodium Formation. *Sci. Rep.* **2016**, *6*, 37874. [[CrossRef](#)]
131. Oser, M.; Dovas, A.; Cox, D.; Condeelis, J. Nck1 and Grb2 Localization Patterns Can Distinguish Invadopodia from Podosomes. *Eur. J. Cell Biol.* **2011**, *90*, 181–188. [[CrossRef](#)]
132. Weidmann, M.D.; Surve, C.R.; Eddy, R.J.; Chen, X.; Gertler, F.B.; Sharma, V.P.; Condeelis, J.S. Mena(INV) Dysregulates Cortactin Phosphorylation to Promote Invadopodium Maturation. *Sci. Rep.* **2016**, *6*, 36142. [[CrossRef](#)] [[PubMed](#)]
133. Hughes, S.K.; Oudin, M.J.; Tadros, J.; Neil, J.; Del Rosario, A.; Joughin, B.A.; Ritsma, L.; Wyckoff, J.; Vasile, E.; Eddy, R.; et al. PTP1B-Dependent Regulation of Receptor Tyrosine Kinase Signaling by the Actin-Binding Protein Mena. *MBoC* **2015**, *26*, 3867–3878. [[CrossRef](#)]
134. Rajadurai, C.V.; Havrylov, S.; Coelho, P.P.; Ratcliffe, C.D.H.; Zaoui, K.; Huang, B.H.; Monast, A.; Chughtai, N.; Sangwan, V.; Gertler, F.B.; et al. 5'-Inositol Phosphatase SHIP2 Recruits Mena to Stabilize Invadopodia for Cancer Cell Invasion. *J. Cell Biol.* **2016**, *214*, 719–734. [[CrossRef](#)]
135. Gorai, S.; Paul, D.; Haloi, N.; Borah, R.; Santra, M.K.; Manna, D. Mechanistic Insights into the Phosphatidylinositol Binding Properties of the Pleckstrin Homology Domain of Lamellipodin. *Mol. Biosyst.* **2016**, *12*, 747–757. [[CrossRef](#)] [[PubMed](#)]
136. Bravo-Cordero, J.J.; Magalhaes, M.A.O.; Eddy, R.J.; Hodgson, L.; Condeelis, J. Functions of Cofilin in Cell Locomotion and Invasion. *Nat. Rev. Mol. Cell Biol.* **2013**, *14*, 405–415. [[CrossRef](#)]
137. Beaty, B.T.; Condeelis, J. Digging a Little Deeper: The Stages of Invadopodium Formation and Maturation. *Eur. J. Cell Biol.* **2014**, *93*, 438–444. [[CrossRef](#)]
138. Watson, J.R.; Owen, D.; Mott, H.R. Cdc42 in Actin Dynamics: An Ordered Pathway Governed by Complex Equilibria and Directional Effector Handover. *Small GTPases* **2017**, *8*, 237–244. [[CrossRef](#)] [[PubMed](#)]
139. Murphy, D.A.; Courtneidge, S.A. The “ins” and “outs” of Podosomes and Invadopodia: Characteristics, Formation and Function. *Nat. Rev. Mol. Cell Biol.* **2011**, *12*, 413–426. [[CrossRef](#)]
140. Jacob, A.; Linklater, E.; Bayless, B.A.; Lyons, T.; Prekeris, R. The Role and Regulation of Rab40b-Tks5 Complex during Invadopodia Formation and Cancer Cell Invasion. *J. Cell Sci.* **2016**, *129*, 4341–4353. [[CrossRef](#)]
141. Williams, K.C.; McNeilly, R.E.; Coppelino, M.G. SNAP23, Syntaxin4, and Vesicle-Associated Membrane Protein 7 (VAMP7) Mediate Trafficking of Membrane Type 1-Matrix Metalloproteinase (MT1-MMP) during Invadopodium Formation and Tumor Cell Invasion. *Mol. Biol. Cell.* **2014**, *25*, 2061–2070. [[CrossRef](#)]
142. Steffen, A.; Le Dez, G.; Poincloux, R.; Recchi, C.; Nassoy, P.; Rottner, K.; Galli, T.; Chavrier, P. MT1-MMP-Dependent Invasion Is Regulated by TI-VAMP/VAMP7. *Curr. Biol.* **2008**, *18*, 926–931. [[CrossRef](#)]
143. Vieira, L.F.D.A.; Lins, M.P.; Viana, I.M.M.N.; Dos Santos, J.E.; Smaniotto, S.; Reis, M.D.D.S. Metallic Nanoparticles Reduce the Migration of Human Fibroblasts In Vitro. *Nanoscale Res. Lett.* **2017**, *12*, 200. [[CrossRef](#)]
144. Lo, H.-M.; Ma, M.-C.; Shieh, J.; Chen, H.-L.; Wu, W. Naked Physically Synthesized Gold Nanoparticles Affect Migration, Mitochondrial Activity, and Proliferation of Vascular Smooth Muscle Cells. *Int. J. Nanomed.* **2018**, *13*, 3163–3176. [[CrossRef](#)] [[PubMed](#)]
145. Kráľovec, K.; Havelek, R.; Koutová, D.; Veverka, P.; Kubíčková, L.; Brázda, P.; Kohout, J.; Herynek, V.; Vosmanská, M.; Kaman, O. Magnetic Nanoparticles of Ga-Substituted ϵ -Fe₂O₃ for Biomedical Applications: Magnetic Properties, Transverse Relaxivity, and Effects of Silica-Coated Particles on Cytoskeletal Networks. *J. Biomed. Mater. Res. Part A* **2020**, *108*, 1563–1578. [[CrossRef](#)] [[PubMed](#)]
146. Sheykhzadeh, S.; Luo, M.; Peng, B.; White, J.; Abdalla, Y.; Tang, T.; Mäkilä, E.; Voelcker, N.H.; Tong, W.Y. Transferrin-Targeted Porous Silicon Nanoparticles Reduce Glioblastoma Cell Migration across Tight Extracellular Space. *Sci. Rep.* **2020**, *10*, 2320. [[CrossRef](#)]
147. Popara, J.; Accomasso, L.; Vitale, E.; Gallina, C.; Roggio, D.; Iannuzzi, A.; Raimondo, S.; Rastaldo, R.; Alberto, G.; Catalano, F.; et al. Silica Nanoparticles Actively Engage with Mesenchymal Stem Cells in Improving Acute Functional Cardiac Integration. *Nanomedicine* **2018**, *13*, 1121–1138. [[CrossRef](#)] [[PubMed](#)]
148. Kenific, C.M.; Wittmann, T.; Debnath, J. Autophagy in Adhesion and Migration. *J. Cell Sci.* **2016**, *129*, 3685–3693. [[CrossRef](#)] [[PubMed](#)]
149. Sharifi, M.N.; Mowers, E.E.; Drake, L.E.; Collier, C.; Chen, H.; Zamora, M.; Mui, S.; Macleod, K.F. Autophagy Promotes Focal Adhesion Disassembly and Cell Motility of Metastatic Tumor Cells through the Direct Interaction of Paxillin with LC3. *Cell Rep.* **2016**, *15*, 1660–1672. [[CrossRef](#)] [[PubMed](#)]

150. Kenific, C.M.; Stehbens, S.J.; Goldsmith, J.; Leidal, A.M.; Faure, N.; Ye, J.; Wittmann, T.; Debnath, J. NBR1 Enables Autophagy-Dependent Focal Adhesion Turnover. *J. Cell Biol.* **2016**, *212*, 577–590. [[CrossRef](#)]
151. Dower, C.M.; Wills, C.A.; Frisch, S.M.; Wang, H.-G. Mechanisms and Context Underlying the Role of Autophagy in Cancer Metastasis. *Autophagy* **2018**, *14*, 1110–1128. [[CrossRef](#)] [[PubMed](#)]
152. Wang, Y.; Yin, S.; Zhang, L.; Shi, K.; Tang, J.; Zhang, Z.; He, Q. A Tumor-Activatable Particle with Antimetastatic Potential in Breast Cancer via Inhibiting the Autophagy-Dependent Disassembly of Focal Adhesion. *Biomaterials* **2018**, *168*, 1–9. [[CrossRef](#)]
153. Shin, T.H.; Lee, D.Y.; Ketebo, A.A.; Lee, S.; Manavalan, B.; Basith, S.; Ahn, C.; Kang, S.H.; Park, S.; Lee, G. Silica-Coated Magnetic Nanoparticles Decrease Human Bone Marrow-Derived Mesenchymal Stem Cell Migratory Activity by Reducing Membrane Fluidity and Impairing Focal Adhesion. *Nanomaterials* **2019**, *9*, 1475. [[CrossRef](#)]
154. Mulens-Arias, V.; Rojas, J.M.; Sanz-Ortega, L.; Portilla, Y.; Pérez-Yagüe, S.; Barber, D.F. Polyethylenimine-Coated Superparamagnetic Iron Oxide Nanoparticles Impair in Vitro and in Vivo Angiogenesis. *Nanomed. Nanotechnol. Biol. Med.* **2019**, *21*, 102063. [[CrossRef](#)] [[PubMed](#)]
155. Ma, X.; Hartmann, R.; De Aberasturi, D.J.; Yang, F.; Soenen, S.J.H.; Manshian, B.B.; Franz, J.; Valdeperez, D.; Pelaz, B.; Feliu, N.; et al. Colloidal Gold Nanoparticles Induce Changes in Cellular and Subcellular Morphology. *ACS Nano* **2017**, *11*, 7807–7820. [[CrossRef](#)]
156. Kráľovec, K.; Melounková, L.; Slováková, M.; Mannová, N.; Sedlák, M.; Bartáček, J.; Havelek, R. Disruption of Cell Adhesion and Cytoskeletal Networks by Thiol-Functionalized Silica-Coated Iron Oxide Nanoparticles. *Int. J. Mol. Sci.* **2020**, *21*, 9350. [[CrossRef](#)] [[PubMed](#)]
157. Ketebo, A.A.; Shin, T.H.; Jun, M.; Lee, G.; Park, S. Effect of Silica-Coated Magnetic Nanoparticles on Rigidity Sensing of Human Embryonic Kidney Cells. *J. Nanobiotechnology* **2020**, *18*, 170. [[CrossRef](#)] [[PubMed](#)]
158. Marcus, J.; Bejerano-Sagie, M.; Patterson, N.; Bagchi, S.; Verkhusha, V.V.; Connolly, D.; Goldberg, G.L.; Golden, A.; Sharma, V.P.; Condeelis, J.; et al. Septin 9 Isoforms Promote Tumorigenesis in Mammary Epithelial Cells by Increasing Migration and ECM Degradation through Metalloproteinase Secretion at Focal Adhesions. *Oncogene* **2019**, *38*, 5839. [[CrossRef](#)]
159. Mulens-Arias, V.; Balfourier, A.; Nicolás-Boluda, A.; Carn, F.; Gazeau, F. Disturbance of Adhesomes by Gold Nanoparticles Reveals a Size- and Cell Type-Bias. *Biomater. Sci.* **2019**, *7*, 389–408. [[CrossRef](#)]
160. Soenen, S.J.H.; Nuytten, N.; De Meyer, S.F.; De Smedt, S.C.; De Cuyper, M. High Intracellular Iron Oxide Nanoparticle Concentrations Affect Cellular Cytoskeleton and Focal Adhesion Kinase-Mediated Signaling. *Small* **2010**, *6*, 832–842. [[CrossRef](#)] [[PubMed](#)]
161. Tay, C.Y.; Cai, P.; Setyawati, M.I.; Fang, W.; Tan, L.P.; Hong, C.H.L.; Chen, X.; Leong, D.T. Nanoparticles Strengthen Intracellular Tension and Retard Cellular Migration. *Nano Lett.* **2014**, *14*, 83–88. [[CrossRef](#)]
162. Discher, D.E.; Janmey, P.; Wang, Y. Tissue Cells Feel and Respond to the Stiffness of Their Substrate. *Science* **2005**, *310*, 1139–1143. [[CrossRef](#)]
163. Ingber, D.E. Tensegrity: The Architectural Basis of Cellular Mechanotransduction. *Annu. Rev. Physiol.* **1997**, *59*, 575–599. [[CrossRef](#)] [[PubMed](#)]
164. Humphrey, J.D.; Dufresne, E.R.; Schwartz, M.A. Mechanotransduction and Extracellular Matrix Homeostasis. *Nat. Rev. Mol. Cell Biol.* **2014**, *15*, 802–812. [[CrossRef](#)]
165. Fouchard, J.; Bimbard, C.; Bufi, N.; Durand-Smet, P.; Proag, A.; Richert, A.; Cardoso, O.; Asnacios, A. Three-Dimensional Cell Body Shape Dictates the Onset of Traction Force Generation and Growth of Focal Adhesions. *Proc. Natl. Acad. Sci. USA* **2014**, *111*, 13075–13080. [[CrossRef](#)] [[PubMed](#)]
166. Wu, Z.; Plotnikov, S.V.; Moalim, A.Y.; Waterman, C.M.; Liu, J. Two Distinct Actin Networks Mediate Traction Oscillations to Confer Focal Adhesion Mechanosensing. *Biophys. J.* **2017**, *112*, 780–794. [[CrossRef](#)]
167. Ibrahim, M.; Schoelermann, J.; Mustafa, K.; Cimpan, M.R. TiO₂ Nanoparticles Disrupt Cell Adhesion and the Architecture of Cytoskeletal Networks of Human Osteoblast-like Cells in a Size Dependent Manner. *J. Biomed. Mater. Res. Part A* **2018**, *106*, 2582–2593. [[CrossRef](#)]
168. Miyauchi, T.; Yamada, M.; Yamamoto, A.; Iwasa, F.; Suzawa, T.; Kamijo, R.; Baba, K.; Ogawa, T. The Enhanced Characteristics of Osteoblast Adhesion to Photofunctionalized Nanoscale TiO₂ Layers on Biomaterials Surfaces. *Biomaterials* **2010**, *31*, 3827–3839. [[CrossRef](#)]
169. Lipski, A.M.; Pino, C.J.; Haselton, F.R.; Chen, I.-W.; Shastri, V.P. The Effect of Silica Nanoparticle-Modified Surfaces on Cell Morphology, Cytoskeletal Organization and Function. *Biomaterials* **2008**, *29*, 3836–3846. [[CrossRef](#)]
170. Perez, J.E.; Fage, F.; Pereira, D.; Abou-Hassan, A.; Asnacios, S.; Asnacios, A.; Wilhelm, C. Transient Cell Stiffening Triggered by Magnetic Nanoparticle Exposure. *J. Nanobiotechnol.* **2021**, *19*, 117. [[CrossRef](#)] [[PubMed](#)]
171. Lyu, Z.; Wang, H.; Wang, Y.; Ding, K.; Liu, H.; Yuan, L.; Shi, X.; Wang, M.; Wang, Y.; Chen, H. Maintaining the Pluripotency of Mouse Embryonic Stem Cells on Gold Nanoparticle Layers with Nanoscale but Not Microscale Surface Roughness. *Nanoscale* **2014**, *6*, 6959. [[CrossRef](#)]
172. Chen, W.; Villa-Diaz, L.G.; Sun, Y.; Weng, S.; Kim, J.K.; Lam, R.H.W.; Han, L.; Fan, R.; Krebsbach, P.H.; Fu, J. Nanotopography Influences Adhesion, Spreading, and Self-Renewal of Human Embryonic Stem Cells. *ACS Nano* **2012**, *6*, 4094–4103. [[CrossRef](#)]
173. Azatov, M.; Sun, X.; Suberi, A.; Fourkas, J.T.; Upadhyaya, A. Topography on a Subcellular Scale Modulates Cellular Adhesions and Actin Stress Fiber Dynamics in Tumor Associated Fibroblasts. *Phys. Biol.* **2017**, *14*, 065003. [[CrossRef](#)]

174. Bello, D.G.; Fouillen, A.; Badia, A.; Nanci, A. A Nanoporous Titanium Surface Promotes the Maturation of Focal Adhesions and Formation of Filopodia with Distinctive Nanoscale Protrusions by Osteogenic Cells. *Acta Biomater.* **2017**, *60*, 339–349. [[CrossRef](#)] [[PubMed](#)]
175. Arnold, M.; Schwieder, M.; Blümmel, J.; Cavalcanti-Adam, E.A.; López-García, M.; Kessler, H.; Geiger, B.; Spatz, J.P. Cell Interactions with Hierarchically Structured Nano-Patterned Adhesive Surfaces. *Soft Matter* **2009**, *5*, 72–77. [[CrossRef](#)] [[PubMed](#)]
176. Abagnale, G.; Steger, M.; Nguyen, V.H.; Hersch, N.; Sechi, A.; Joussen, S.; Denecke, B.; Merkel, R.; Hoffmann, B.; Dreser, A.; et al. Surface Topography Enhances Differentiation of Mesenchymal Stem Cells towards Osteogenic and Adipogenic Lineages. *Biomaterials* **2015**, *61*, 316–326. [[CrossRef](#)]
177. Posa, F.; Baha-Schwab, E.H.; Wei, Q.; Di Benedetto, A.; Neubauer, S.; Reichart, F.; Kessler, H.; Spatz, J.P.; Albiges-Rizo, C.; Mori, G.; et al. Surface Co-Presentation of BMP-2 and Integrin Selective Ligands at the Nanoscale Favors A5 β 1 Integrin-Mediated Adhesion. *Biomaterials* **2021**, *267*, 120484. [[CrossRef](#)]
178. Kang, H.; Wong, D.S.H.; Yan, X.; Jung, H.J.; Kim, S.; Lin, S.; Wei, K.; Li, G.; Dravid, V.P.; Bian, L. Remote Control of Multimodal Nanoscale Ligand Oscillations Regulates Stem Cell Adhesion and Differentiation. *ACS Nano* **2017**, *11*, 9636–9649. [[CrossRef](#)]
179. Kang, H.; Jung, H.J.; Wong, D.S.H.; Kim, S.K.; Lin, S.; Chan, K.F.; Zhang, L.; Li, G.; Dravid, V.P.; Bian, L. Remote Control of Heterodimeric Magnetic Nanoswitch Regulates the Adhesion and Differentiation of Stem Cells. *J. Am. Chem. Soc.* **2018**, *140*, 5909–5913. [[CrossRef](#)]
180. Okada, T.; Ogura, T. Nanoscale Imaging of the Adhesion Core Including Integrin B1 on Intact Living Cells Using Scanning Electron-Assisted Dielectric-Impedance Microscopy. *PLoS ONE* **2018**, *13*, e0204133. [[CrossRef](#)]
181. Rojas, J.M.; Sanz-Ortega, L.; Mulens-Arias, V.; Gutiérrez, L.; Pérez-Yagüe, S.; Barber, D.F. Superparamagnetic Iron Oxide Nanoparticle Uptake Alters M2 Macrophage Phenotype, Iron Metabolism, Migration and Invasion. *Nanomed. Nanotechnol. Biol. Med.* **2016**, *12*, 1127–1138. [[CrossRef](#)] [[PubMed](#)]
182. Mulens-Arias, V.; Rojas, J.M.; Pérez-Yagüe, S.; Morales, M.P.; Barber, D.F. Polyethylenimine-Coated SPIONs Trigger Macrophage Activation through TLR-4 Signaling and ROS Production and Modulate Podosome Dynamics. *Biomaterials* **2015**, *52*, 494–506. [[CrossRef](#)]
183. Akatsuka, S.; Yamashita, Y.; Ohara, H.; Liu, Y.-T.; Izumiya, M.; Abe, K.; Ochiai, M.; Jiang, L.; Nagai, H.; Okazaki, Y.; et al. Fenton Reaction Induced Cancer in Wild Type Rats Recapitulates Genomic Alterations Observed in Human Cancer. *PLoS ONE* **2012**, *7*, e43403. [[CrossRef](#)] [[PubMed](#)]
184. Brillo, V.; Chierigato, L.; Leanza, L.; Muccioli, S.; Costa, R. Mitochondrial Dynamics, ROS, and Cell Signaling: A Blended Overview. *Life* **2021**, *11*, 332. [[CrossRef](#)]
185. Xu, J.; Yang, J.; Nyga, A.; Ehteramy, M.; Moraga, A.; Wu, Y.; Zeng, L.; Knight, M.M.; Shelton, J.C. Cobalt (II) Ions and Nanoparticles Induce Macrophage Retention by ROS-Mediated down-Regulation of RhoA Expression. *Acta Biomater.* **2018**, *72*, 434–446. [[CrossRef](#)] [[PubMed](#)]
186. Linder, S.; Aepfelbacher, M. Podosomes: Adhesion Hot-Spots of Invasive Cells. *Trends Cell Biol.* **2003**, *13*, 376–385. [[CrossRef](#)]
187. Mulens-Arias, V.; Rojas, J.M.; Pérez-Yagüe, S.; Morales, M.d.P.; Barber, D.F. Polyethylenimine-Coated SPION Exhibits Potential Intrinsic Anti-Metastatic Properties Inhibiting Migration and Invasion of Pancreatic Tumor Cells. *J. Control. Release* **2015**, *216*, 78–92. [[CrossRef](#)]
188. Simone, T.M.; Higgins, C.E.; Czekay, R.-P.; Law, B.K.; Higgins, S.P.; Archambeault, J.; Kutz, S.M.; Higgins, P.J. SERPINE1: A Molecular Switch in the Proliferation-Migration Dichotomy in Wound-“Activated” Keratinocytes. *Adv. Wound Care* **2014**, *3*, 281–290. [[CrossRef](#)]
189. Shih, Y.-P.; Takada, Y.; Lo, S.H. Silencing of DLC1 Upregulates PAI-1 Expression and Reduces Migration in Normal Prostate Cells. *Mol. Cancer Res.* **2012**, *10*, 34–39. [[CrossRef](#)]